3

Behavior of Dielectrics in Alternating Fields

In this chapter we shall discuss the essential aspects of the behavior of dielectric materials when subjected to alternating fields. The discussion is based on the atomic models employed in the preceding chapter, and from the behavior of these models in alternating fields we shall arrive at the frequency dependence of the macroscopic dielectric constant. As a result of the discussion it will become evident that the dielectric constant under these conditions is in general a *complex quantity* of which the imaginary part is a measure for the *dielectric losses* of the material. The discussion in this chapter is by no means complete and serves mainly to illustrate the principles leading to the complex dielectric constant and its interpretation.

3.1 Frequency dependence of the electronic polarizability

Let us return at this point to the atomic model employed in section 2.3, and let us inquire what results would be obtained for the polarizability α_e when the model is subjected to an alternating field. For simplicity we shall assume a nucleus of charge $+e$ and a single electron, the latter being represented by an electron cloud of total charge $-e$ distributed homogeneously through the volume of a sphere of radius R; the center of the sphere in the absence of an external field coincides with the nucleus (see Fig. 2.5). Since the nucleus is much heavier than the electron cloud, we may consider the nucleus to a good approximation to be at rest, the electron cloud carrying

out the motion forced on it by the a-c field. The first problem is, of course, to set up the differential equation which describes the motion of the electron cloud. First consider the following problem: suppose the electron cloud is displaced by an amount x_0 relative to the nucleus and then the system is left to itself. What is the differential equation which describes the motion of the electron cloud under these circumstances? From the discussion in section (2.3) it follows that the force which tends to drive the center of the cloud to the nucleus is given by

$$F = -e^2x/4\pi\epsilon_0R^3 = -ax \tag{3.1}$$

where x is the displacement. The force F is called the *restoring force* and a the *restoring force constant*. Hence, if there were no damping, and in the absence of an applied field, the equation of motion of the electron cloud would be identical with that for a *harmonic oscillator*, viz.,

$$m\frac{d^2x}{dt^2} = -ax \tag{3.2}$$

where m is the mass of the cloud, i.e. the electron mass. It is well known that the solution of (3.2) is

$$x = x_0 \sin(\omega_0 t + \delta) \tag{3.3}$$

where x_0 and δ are integration constants, and where $\omega_0 = (a/m)^{1/2}$ is the *natural* or *resonance angular frequency*. An estimate of the order of magnitude of ω_0 is obtained by putting in (3.1) $R \cong 10^{-10}$ m; this gives with $m = 0.9 \times 10^{-31}$ kg a value of $\omega_0 \cong 10^{16}$ radians sec^{-1}. Hence, the frequencies we are talking about lie in the *ultraviolet* part of the electromagnetic spectrum.

Expression (3.2) is incomplete in the sense that it does not take into account the emission of electromagnetic radiation by the system; the emission results from the time variation of the acceleration of the electron cloud and leads to *damping*. In the mechanical case, damping of the oscillating particle would result from the viscosity of the medium in which the particle moves and it is well known that this damping leads to a term proportional to the *velocity* of the particle in the equation of motion. It can be shown that, in the electrical case under consideration, the damping due to radiation may be represented in a similar way; i.e., instead of (3.2) we should write

$$m\frac{d^2x}{dt^2} = -ax - 2b\frac{dx}{dt} \tag{3.4}$$

where the last term is the damping term. The constant b is related to the natural frequency ω_0 in the following manner

$$2b = \mu_0 e^2\omega_0^2/6\pi mc \tag{3.5}$$

where $\mu_0 = 1.257 \times 10^{-6}$ henry m^{-1} is the magnetic permeability of vacuum, and $c = 2.9979 \times 10^8$ m sec^{-1} is the speed of light. Substituting numerical values, the reader may verify that $2b/m \ll \omega_0$, a result which will be used later.

We are now in a position to write down the equation of motion of the electron cloud in the presence of an alternating external field. Let the field be applied in the x-direction and let it be represented by $E_0 \cos \omega t$, ω being the angular frequency. The force on the electron cloud resulting from the field is then $-eE_0 \cos \omega t$ and the equation of motion is

$$m \frac{d^2x}{dt^2} = -ax - 2b \frac{dx}{dt} - eE_0 \cos \omega t \tag{3.6}$$

To solve this equation for $x(t)$ it is convenient to use complex notation. Thus, we shall write*

$$E_0 \cos \omega t = \text{Re}\,[E_0 e^{j\omega t}] = E_0 \,\text{Re}\,[e^{j\omega t}] \tag{3.7}$$

and we shall assume the solution to be of the form

$$x(t) = \text{Re}\,[A^* e^{j\omega t}] \tag{3.8}$$

where A^* is in general a complex amplitude. Substituting the last two expressions into (3.6) one obtains

$$\text{Re}\left\{\left[-\omega^2 A^* + \frac{a}{m} A^* + j \frac{2b\omega}{m} A^* + \frac{e}{m} E_0\right] e^{j\omega t}\right\} = 0$$

From this it follows that the expression in square brackets is zero; writing $a/m = \omega_0^2$ in accordance with the definition of the natural frequency ω_0, we find

$$A^* = \frac{(e/m)E_0}{\omega^2 - \omega_0^2 - j(2b/m)} \tag{3.9}$$

What is the induced dipole moment as function of time? In general, $\mu_{\text{ind}}(t) = -ex(t)$ so that we find from (3.8) and (3.9)

$$\mu_{\text{ind}}(t) = \text{Re}\left[\frac{(e^2/m)E_0 e^{j\omega t}}{\omega_0^2 - \omega^2 + j(2b\omega/m)}\right] \tag{3.10}$$

Since the coefficient of $E_0 e^{j\omega t}$ is a complex quantity, we see that the static definition $\mu_{\text{ind}} = \alpha_e E$ cannot be applied in this case. We are therefore compelled to introduce a *complex polarizability* α_e^* by means of the following expression

$$\mu_{\text{ind}}(t) = \text{Re}\,[\alpha_e^* E_0 e^{j\omega t}] \tag{3.11}$$

where

$$\alpha_e^* = \frac{e^2/m}{\omega_0^2 - \omega^2 + j(2b\omega/m)} \tag{3.12}$$

* Re [ ] means "real part of [ ]". Complex quantities will be provided with an asterisk superscript.

Writing out the real and imaginary parts of (3.12) we find

$$\alpha_e^* = \frac{e^2}{m}\left[\frac{\omega_0^2 - \omega^2}{(\omega_0^2 - \omega^2)^2 + (4b^2\omega^2/m^2)} - j\frac{2b\omega/m}{(\omega_0^2 - \omega^2)^2 + (4b^2\omega^2/m^2)}\right]$$
$$= \alpha_e' - j\alpha_e'' \tag{3.13}$$

where α_e' and α_e'' represent, respectively, the real and imaginary parts of the polarizability.

We shall now discuss the frequency dependence of the real and imaginary parts of α_e^*, referring to Fig. 3.1. First of all, we note that for $\omega = 0$

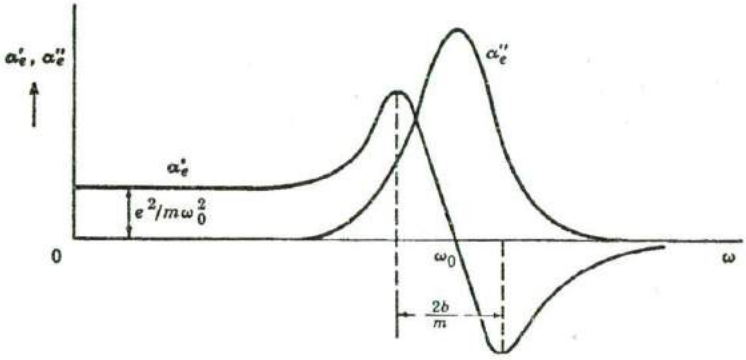

Fig. 3.1. Schematic representation of the frequency dependence of the real and imaginary parts α_e' and α_e'', respectively, of the electronic polarizability for a single electron.

the imaginary part vanishes, the real part being equal to the *static value* $e^2/m\omega_0^2$. The real part is positive for all values $\omega < \omega_0$ and negative for all values $\omega > \omega_0$; the real part is zero for $\omega = \omega_0$. Remembering that $2b \ll \omega_0$, it is noted that α_e' is essentially constant from zero frequency up to frequencies which become comparable to ω_0. In the region where ω is nearly equal to ω_0, the behavior can be discussed conveniently by introducing the variable

$$\Delta\omega = \omega_0 - \omega \quad \text{with} \quad \Delta\omega \ll \omega_0$$

We may then write approximately

$$\omega_0^2 - \omega^2 = (\omega_0 + \omega)(\omega_0 - \omega) \cong 2\omega_0\Delta\omega$$

and the real part becomes

$$\alpha_e' \cong \frac{e^2}{m}\frac{2\omega_0\Delta\omega}{4\omega_0^2(\Delta\omega)^2 + 4b^2\omega_0^2/m^2} = \frac{e^2}{m}\frac{(\Delta\omega)/2\omega_0}{(\Delta\omega)^2 + b^2/m^2} \tag{3.14}$$

This expression has a maximum for $\Delta\omega = b/m$ and a minimum for $\Delta\omega = -b/m$, as illustrated in Fig. 3.1. The dampings coefficient $2b$ is thus a

measure for the distance between the maximum and minimum in the *dispersion curve* (α_e' versus ω).

The imaginary part α_e'' vanishes for $\omega = 0$ as well as for $\omega \to \infty$. In the vicinity of $\omega = \omega_0$, we may write by introducing the variable $\Delta\omega$,

$$\alpha_e'' \cong \frac{e^2 b/2m^2\omega_0}{(\Delta\omega)^2 + b^2/m^2} \tag{3.14a}$$

Thus, α_e'' exhibits a maximum for $\Delta\omega = 0$, i.e. for $\omega = \omega_0$; the magnitude of the maximum is $(\alpha_e'')_{max} = e^2/2\omega_0 b$. The width of the bell-shaped curve for α_e'' corresponding to half the maximum value is readily found to be $2b/m$.

The consequences of a complex electronic polarizability for the dielectric behavior will be discussed later, but it may be said here already that the *imaginary part of the polarizability gives rise to absorption of energy by the system from the field.*

The model discussed above was limited to the existence of one electron. In general an atom contains a number of electrons, each of them corresponding to a particular force constant a_i and a particular damping constant b_i. Consequently, the atom in general will have a series of ω_{0i} values

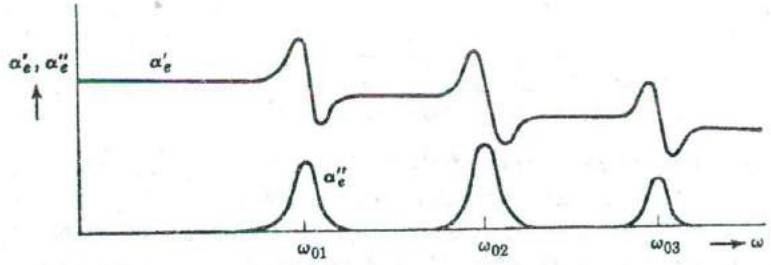

Fig. 3.2. Schematic representation of the frequency dependence of the real and imaginary parts of the polarizability of an atom; in this case there are a series of resonance frequencies ω_{01}, ω_{02}, etc.

and the polarizability will exhibit a frequency dependence as indicated schematically in Fig. 3.2.

3.2 Ionic polarization as a function of frequency

The frequency dependence of the ionic polarizability can be discussed in complete analogy with the electronic polarizability, the difference between the two cases being of a quantitative nature only. When two ions in a molecule or solid are displaced relative to each other, the restoring

force which tends to drive them back to their equilibrium positions is to a good approximation proportional to the displacement. Hence, the forces are harmonic. The masses of the particles in the present case are, of course, those of atoms rather than of electrons. As a result, the natural frequencies of the ionic vibrations lie in the *infrared* part of the electromagnetic spectrum, corresponding to $\omega_0 \approx 10^{14}$ radians per second. Thus, the ionic polarizability of a molecule will also be a complex quantity which may be written in the form

$$\alpha_i^* = \alpha_i' - j\alpha_i'' \tag{3.15}$$

The real part α_i' as a function of the frequency ω of an applied field exhibits the same features as those represented for α_e' in Fig. 3.2; the only difference is that the ω_{0i} values for which the maxima and minima occur are now displaced to the infrared region. Similarly, α_i'' as a function of frequency will exhibit various bell-shaped maxima, one for each of the characteristic frequencies ω_{0i}.

3.3 The complex dielectric constant of non-dipolar solids

On the basis of the information obtained in the preceding two sections, let us consider the frequency dependence of the dielectric constant of a solid, assuming the solid contains no permanent dipoles. The last restriction is not particularly severe in the case of solids, because usually the dipoles are not able to rotate anyway. In the solid state, and also in the liquid state, the applied field must be replaced by the *internal* field E_i, as discussed in section 2.6. For simplicity we shall assume that the internal field is given by the Lorentz field (2.33), so that

$$E_i(t) = E(t) + P(t)/3\epsilon_0 \tag{3.16}$$

where $P(t)$ is the electric dipole moment per unit volume at the instant t. Let us assume that the solid contains N units per m^3 from which the solid may be built up by a three-dimensional stacking. Let each of these units be characterized by an electronic polarizability α_e^* and an ionic polarizability α_i^*. In accordance with (3.11) we may then write

$$P(t) = N \operatorname{Re}\left[(\alpha_e^* + \alpha_i^*)E_{0i}^* e^{j\omega t}\right] \tag{3.17}$$

where E_{0i}^* is the complex amplitude of the internal field; ω is the frequency of the applied field. Note that in general, $P(t)$ *will not be in phase with the applied field, or with the internal field.* Consequently, the relationship derived for static fields [see (2.9)]:

$$P = \epsilon_0(\epsilon_r - 1)E$$

is not valid in the case of an alternating field, and we shall therefore define a *complex relative dielectric constant* ϵ_r^* such that

$$P(t) = \epsilon_0 \operatorname{Re}\left[(\epsilon_r^* - 1)E_0 e^{j\omega t}\right] \tag{3.18}$$

where it has been assumed that the applied field is given by $E_0 \cos \omega t$. Note that by introducing the complex ϵ_r^*, we have introduced the possibility of a phase difference between $P(t)$ and $E(t)$. Substituting (3.18) into (3.16) we may then write

$$E_i(t) = \operatorname{Re}\left[\frac{(\epsilon_r^* + 2)}{3} E_0 e^{j\omega t}\right] = \operatorname{Re}\left[E_{0i}^* e^{j\omega t}\right] \tag{3.19}$$

Equating (3.17) and (3.18), and substituting (3.19) into (3.17) we find

$$\frac{\epsilon_r^* - 1}{\epsilon_r^* + 2} = \frac{1}{3\epsilon_0} N(\alpha_e^* + \alpha_i^*) \tag{3.20}$$

The reader may compare this result with the Clausius-Mosotti expression (2.38) derived for the static case under the same assumption, viz. a Lorentz field for E_i.

The main point of the present discussion is this: the complex dielectric constant of non-dipolar solids is determined by the complex polarizabilities α_e^* and α_i^*. Consequently, the behavior of the real and imaginary parts of the polarizabilities as function of frequency will be reflected in the frequency dependence of the dielectric constant. One thus arrives at the conclusion that the real and imaginary parts of ϵ_r^* defined by

$$\epsilon_r^* = \epsilon_r' - j\epsilon_r'' \tag{3.21}$$

are functions of the frequency of the applied field, and that these functions are determined by $\alpha_e^*(\omega)$ and $\alpha_i^*(\omega)$.

What practical value do these results have for the electrical engineer? This depends on the frequency range in which one happens to be interested. According to the preceding sections, α_e^* and α_i^* are real as long as the frequencies lie below infrared frequencies. Hence, up to microwaves, ϵ_r^* is essentially real for the materials under discussion and their behavior is the same as it is in static fields. The solids discussed here, however, are idealized in the sense that many of them contain ions which may be displaced over one or more interatomic distances under influence of an external field; this is the case, for example, in glassy materials, and to some extent even in crystalline materials. Such processes may lead to an imaginary part of the dielectric constant, and to dielectric losses as will be seen in subsequent sections.

3.4 Dipolar relaxation

So far in this chapter we have discussed only the frequency dependence of the electronic and ionic polarization. From the electrical engineering point of view, the *frequency dependence of the orientational polarization* in liquids and glassy substances is perhaps of greater importance, since it gives rise to dielectric losses in the frequency range between zero and many thousand megacycles, depending upon the substance. Although the discussion refers in particular to permanent dipoles rotating in liquids, the results have much wider applicability.

Consider a liquid containing N permanent dipoles μ_p per unit volume. Suppose it has been subjected for a long time to a d-c field E; let the orientational polarization in equilibrium with the field be P_o. When at the instant $t = 0$ the field is suddenly switched off, the polarization will not instantaneously become zero, because there is a certain time required for the rotation of the dipoles. Without going into the details of the molecular processes involved, we shall assume that the polarization as function of time decays to zero in accordance with the formula (see Fig. 3.3a)

$$P_o(t) = P_o e^{-t/\tau} \tag{3.22}$$

The quantity τ has the dimensions of time and is called the *relaxation time*. In a liquid, τ increases as the viscosity of the liquid increases, as one would

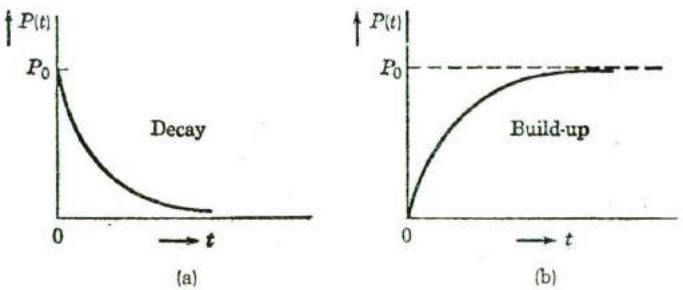

Fig. 3.3. Illustrating in (a) the decay of the orientational polarization of a liquid upon switching-off the field at $t = 0$. In (b) a field is switched on at $t = 0$; the curve represents the growth of the orientational polarization with time.

expect from qualitative arguments. The rate of change of the polarization is evidently given by

$$\frac{d}{dt} P_o(t) = -\frac{P_o}{\tau} e^{-t/\tau} = -\frac{P_o(t)}{\tau} \tag{3.23}$$

Note that the smaller the instantaneous value $P_o(t)$, the smaller the rate at which the decay takes place. Since the ultimate value $P_o(\infty) = 0$, we may also write (3.23) as follows:

$$\frac{d}{dt} P_o(t) = \frac{1}{\tau} [P_o(\infty) - P_o(t)] \tag{3.24}$$

The reason for writing the result in this particular form will become obvious later.

Suppose now that an external field has been absent for a long time, and that at $t = 0$ a field E is switched on. What will $P_o(t)$ be during the build-up to the ultimate equilibrium value P_o? From analogy with similar physical processes the reader will recognize that the answer to this question is [see Fig. 3.3(b)]

$$P_o(t) = P_o(1 - e^{-t/\tau}) \tag{3.25}$$

The rate of increase is then

$$\frac{d}{dt} P_o(t) = \frac{P_o}{\tau} e^{-t/\tau} = \frac{1}{\tau} [P_o - P_o(t)] \tag{3.26}$$

Since $P_o = P_o(\infty)$ in the present case, note that (3.24) and (3.26) have the same form. In other words, *during build-up as well as during decay*, the rate of change of $P_o(t)$ is, apart from the factor $1/\tau$, equal to the ultimate value corresponding to the field E, minus the instantaneous value $P_o(t)$.

The foregoing discussion should be considered as a preparation for the actual question we wish to consider in this section, viz.: given that the equilibrium value of the orientational polarization in a static field E is equal to

$$P_o = \epsilon_0(\epsilon_{r0} - 1)E \tag{3.27}$$

where ϵ_{r0} is that part of the dielectric constant which measures only the orientational polarization, what is $P_o(t)$ when one applies an alternating field $E_0 \cos \omega t$? In order to answer this question, consider expression (3.24), which was found to hold for decay as well as for build-up, and which we shall now assume to hold also in the case of a-c fields. At the instant t, the external field is $E_o \cos \omega t$ and hence at that instant the dipoles are aiming for a $P_o(\infty)$ equal to $\epsilon_0(\epsilon_{r0} - 1)E_0 \cos \omega t$. Consequently, the differential equation for $P_o(t)$ may be written as follows:

$$\frac{d}{dt} P_o(t) = \frac{1}{\tau} [\epsilon_0(\epsilon_{r0} - 1)E_0 \cos \omega t - P_o(t)] \tag{3.28}$$

To solve this equation let us introduce a complex dielectric constant ϵ^*_{r0} [allowing for the possibility of phase differences between $P_o(t)$ and $E(t)$]

by means of the relation

$$P_o(t) = \epsilon_0 \operatorname{Re}\left[(\epsilon_{r0}^* - 1)E_0 e^{j\omega t}\right] \tag{3.29}$$

Substitution into (3.28) then leads to

$$\epsilon_{r0}^* - 1 = \frac{\epsilon_{r0} - 1}{1 + j\omega\tau} \tag{3.30}$$

Hence, for alternating fields, the orientational part of the dielectric constant becomes complex, and is a function of the static value ϵ_{r0} and of $\omega\tau$. Writing out the real and imaginary parts, we obtain

$$\epsilon_{r0}^* - 1 = (\epsilon_{r0} - 1)\left[\frac{1}{1 + \omega^2\tau^2} - j\,\frac{\omega\tau}{1 + \omega^2\tau^2}\right] \tag{3.31}$$

For the polarization we find from (3.29) and (3.31)

$$P_o(t) = \frac{\epsilon_0(\epsilon_{r0} - 1)}{1 + \omega^2\tau^2} E_0 \cos\omega t + \frac{\epsilon_0(\epsilon_{r0} - 1)\omega\tau}{1 + \omega^2\tau^2} E_0 \sin\omega t \tag{3.32}$$

Note that the first term on the right-hand side is in phase with the applied field, whereas the second term lags by 90 degrees. The frequency dependence of the in-phase and the out-of-phase components are represented in Fig. 3.4. It is observed that the in-phase component of $P_o(t)$ begins to dis-

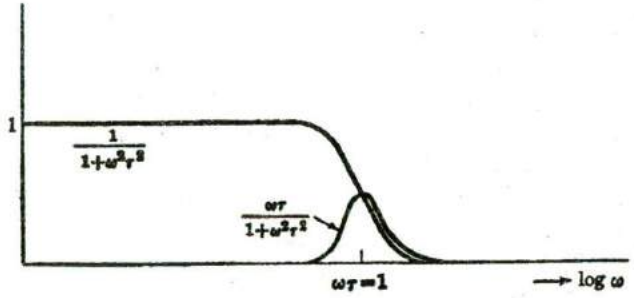

Fig. 3.4. A schematic plot of $1/(1 + \omega^2\tau^2)$ and $\omega\tau/(1 + \omega^2\tau^2)$ as a function of the logarithm of the frequency.

appear when $\omega\tau$ becomes comparable to unity. When $\omega\tau \gg 1$, the dipoles cannot follow the field variations and hence the polarization vanishes. The out-of-phase component of $P_o(t)$ has the same bell shape as the imaginary part of the electronic and ionic polarizabilities, and is a measure for the absorption of energy as we shall see in the next section. By way of illustration we give here some values for τ derived from dielectric measurements for ice and propyl alcohol at various temperatures.

Propyl Alcohol:					
Temp. (°C):	20°	0	−20°	−40°	−60°
$10^{10}\tau$ (sec):	0.9	1.6	3.2	7.4	26

Ice:		
Temp. (°C):	−5°	−22°
$10^{6}\tau$ (sec):	2.7	18

Note that as the temperature is reduced, the relaxation time increases and the frequency for which $\omega\tau = 1$ decreases. Note also that the relaxation time is about 10^4 times as long in ice as in liquid propyl alcohol.

The differential equation for $P_o(t)$, (3.28), also applies to the following situation: With reference to Fig. 3.5 suppose an ion in a particular solid

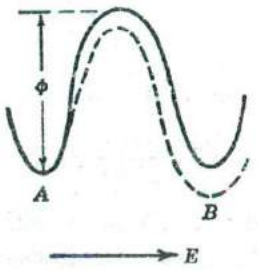

Fig. 3.5. The fully drawn curve represents the potential energy of a positive ion as function of a coordinate which coincides with the line joining two possible positions for the ion, A and B. The dashed curve corresponds to the potential energy in the presence of a field as indicated.

can occupy two positions A and B of equal energy, the two positions being separated by a potential energy barrier ϕ. In the absence of an external field the probability that the particle will be found in A is the same as that for B. When an external field is applied, position B may be preferred if the energy of the particle is lower there than when it resides in A. For a solid containing a significant number of such ions, the process of the ions "jumping" into preferred B-sites may contribute appreciably to the dielectric constant. In an alternating field, these ions will contribute in accordance with the formulas derived above, and τ must then be interpreted as the average time required for an ion to jump from A to B. It can be shown that jumping times of this kind depend on the potential barrier ϕ and on the temperature as follows:

$$\tau = Ae^{\phi/kT} \tag{3.33}$$

where A is a constant; k is Boltzmann's constant ($= 1.38 \times 10^{-23}$ joule per degree. Thus, as T increases, τ decreases, as one would expect from qualitative arguments. In non-crystalline materials such as glasses, it is quite likely that there exists a variety of potential barriers ϕ, and hence a variety of τ-values. Evidence for this will be presented in the next section.

3.5 Dielectric losses

In the preceding sections we have discussed the frequency dependence of the electronic, ionic and orientational contributions to the polarization. Since these contributions are additive, a material may be characterized by a complex dielectric constant

$$\epsilon_r^* = \epsilon_r' - j\epsilon_r'' \tag{3.34}$$

in which the real and imaginary parts ϵ_r' and ϵ_r'' incorporate all three contributions. In the present section we shall show that the imaginary part gives rise to absorption of energy by the material from the alternating field. For this purpose consider a parallel plate condenser filled with a material characterized by ϵ_r^*; the functions $\epsilon_r'(\omega)$ and $\epsilon_r''(\omega)$ are assumed to be given. Let the applied alternating voltage produce a field $E_0 \cos \omega t$. Suppose that at a given instant the charge per unit area on the plates is $\pm Q(t)$. Since the flux density is numerically equal to the charge density, we must have $D(t) = Q(t)$. Also, since the current density is equal to $J(t) = dQ/dt$ we may write

$$J(t) = \frac{dD}{dt} \tag{3.35}$$

On the other hand, since $E(t) = \text{Re}\,[E_0 e^{j\omega t}]$ we may write in accordance with the meaning of the complex dielectric constant

$$D(t) = \text{Re}\,[\epsilon_0 \epsilon_r^* E_0 e^{j\omega t}] = \epsilon_0 E_0\,\text{Re}\,[\epsilon_r^* e^{j\omega t}] \tag{3.36}$$

Substituting (3.34) into this expression we find for the current density from (3.35)

$$\begin{aligned} J(t) &= \epsilon_0 E_0\,\text{Re}\,[(\epsilon_r' - j\epsilon_r'')j\omega e^{j\omega t}] \\ &= \omega\epsilon_0 E_0[\epsilon_r'' \cos \omega t - \epsilon_r' \sin \omega t] \end{aligned} \tag{3.37}$$

Note that the imaginary part ϵ_r'' of the dielectric constant determines the component of the current which is in phase with the applied field. Also, the real part of the dielectric constant, ϵ_r', is coupled with a time factor which is 90 degrees out of phase with the applied field. The reader will readily recognize that, on the average, the last term in (3.37) does not give rise to absorption of energy, whereas the term containing ϵ_r'' does. The instantaneous power per m³ absorbed by the medium is given by $J(t)E(t)$; hence, each second the material absorbs an amount of energy per m³ given by

$$W(t) = \frac{1}{2\pi}\int_0^{2\pi} J(t)E(t)\, d(\omega t) \tag{3.38}$$

Substituting $J(t)$ from (3.37) one readily finds

$$W(t) = (\omega/2)\epsilon_0\epsilon_r'' E_0^2 \tag{3.39}$$

Thus, the *absorption of energy is proportional to the imaginary part of the complex dielectric constant;* whenever there is energy dissipated in the medium we speak of *dielectric losses.*

It follows from (3.37) that a condenser containing a lossy dielectric may be represented by an equivalent circuit which consists of a pure capacitance and a parallel resistance, the latter being inversely proportional to $\epsilon_r''\omega$. It is customary to characterize the losses of a dielectric at a certain frequency and temperature by the so-called *"loss-tangent,"* tan δ, defined as

$$\tan \delta = \epsilon_r''/\epsilon_r' \tag{3.40}$$

The physical meaning of the angle δ may be derived from expression (3.37). If there are no losses, $\epsilon_r'' = 0$ and the current density is then given by $\omega\epsilon_0 E_0\epsilon_r' \cos(\omega t + 90°)$; i.e., the current leads the field by 90 degrees. Under these circumstances $\delta = 0$. If there is a current component in phase with the field, the resulting current will no longer lead the field by 90 degrees but by $90° - \delta$, as indicated in Fig. 3.6.

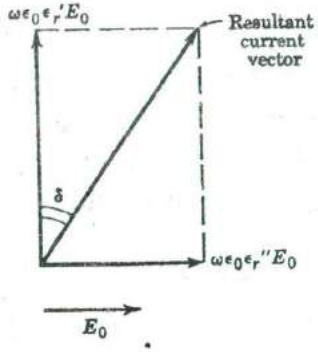

Fig. 3.6. Illustrating the vector relationship between the field vector E_0, the current vector $\omega\epsilon_0\epsilon_r' E_0$ which leads the field by 90 degrees and the current vector $\omega\epsilon_0\epsilon_r'' E_0$ which is in phase with the field. The loss angle δ is indicated.

The dielectric losses in the radio frequency region are usually due to dipole rotation or to ions jumping from one equilibrium position to another. Losses in this region may also be due to a small degree of d-c *conductivity* of the material, but this subject will not be discussed here. The dielectric losses associated with the ionic vibrations, the frequencies of which fall in the infrared region, are usually referred to as *infrared absorption.* Similarly, the losses in the optical region, associated with the electrons, are referred to as *optical absorption.* The occurrence of absorption in the optical region is the source of the color of materials. For example, a crystal of NaCl is transparent in the visible region; this means that there is negligible absorption for the corresponding frequencies. However, after the NaCl has

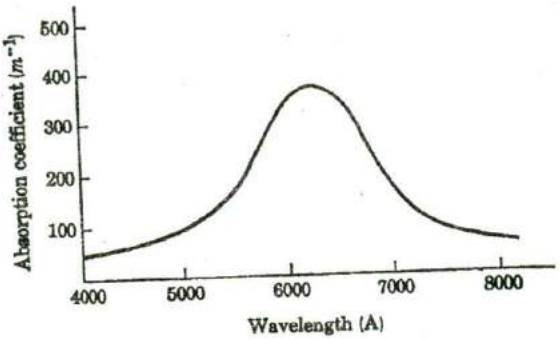

Fig. 3.7. The optical absorption as a function of wavelength resulting from *F*-centers in a KBr crystal, at room temperature. [After A. von Hippel, E. P. Gross, T. G. Telatis, and M. Geller, *Phys. Rev.* **91**, 568 (1953)]

been exposed to X-rays, one finds that it has turned yellow-brown. The reason for this is that, after irradiation with X-rays, a relatively small number of electrons, which have been transferred to positions in the lattice

Table 3.1. THE REAL PART OF THE RELATIVE DIELECTRIC CONSTANT, ϵ_r', AND THE LOSS TANGENT OF VARIOUS DIELECTRICS AT A NUMBER OF FREQUENCIES. (Selected from A. von Hippel, *Dielectric Materials and Applications*)

Material		Frequency in cycles per second 10^2	10^4	10^6	10^8	3×10^9
Pyranol 1467	ϵ_r'	4.42	4.40	4.40	4.08	2.84
	$10^4 \tan \delta$	36	4	25	1300	1200
Cable oil 5314	ϵ_r'	2.25	2.25			2.22
	$10^4 \tan \delta$	3	0.4			18
Teflon	ϵ_r'	2.1	2.1	2.1	2.1	2.1
	$10^4 \tan \delta$	5	3	2	2	1.5
Polystyrene	ϵ_r'	2.59	2.56	2.56	2.55	2.55
	$10^4 \tan \delta$	0.5	0.5	0.7	1.0	3.3
Polyethylene	ϵ_r'	2.25	2.25	2.25	2.25	2.25
	$10^4 \tan \delta$	5	3	4		3
Nylon 66	ϵ_r'	3.88	3.60	3.33	3.16	3.03
	$10^4 \tan \delta$	144	233	257	210	128
Bakelite BM-120	ϵ_r'	4.87	4.62	4.36	3.95	3.70
	$10^4 \tan \delta$	300	200	280	380	438
Glass (Corning 0010)	ϵ_r'	6.68	6.57	6.43	6.33	6.1
	$10^4 \tan \delta$	77	35	16	23	60
Porcelain No. 4462	ϵ_r'	8.99	8.95	8.95	8.95	8.90
	$10^4 \tan \delta$	22	6.0	2.0	4.0	11

where they are not bound so strongly as they were before, give rise to resonance frequencies lying in the visible part of the spectrum. When white light passes through the crystal, a fraction of the light corresponding to a narrow frequency region is absorbed, and the transmitted light is therefore colored. The centers which are responsible for this particular type of absorption are called F-centers (Farbe is the German word for color); they consist of electrons occupying positions in which negative ions are missing. This type of *color center* occurs in all alkali halides as well as in other ionic crystals. An example of F-center absorption in KBr is given in Fig. 3.7; note the bell shape of the curve.

We finally give in Table 3.1 values for the real part of the dielectric constant, ϵ_r', and for tan δ for various materials at a number of frequencies. For a collection of data for a large number of materials, the reader is referred to *Dielectric Materials and Applications*, edited by A. R. von Hippel and cited at the end of the preceding chapter.

References

See those given at the end of Chapter 2.

Problems

3.1 (a) Consider a gas containing N similar atoms per m^3 of a polarizability α. On the basis of expression (3.10) for the induced dipole moment resulting from an alternating field, show that the dielectric constant of the gas is given by

$$\epsilon_r^* = 1 + \frac{Ne^2/m\epsilon_0}{\omega_0^2 - \omega^2 + j2b\omega/m}$$

(b) Consider two parallel metal plates with a separation of 1 m. The space between the plates is occupied by the gas referred to under (a). Show that the admittance per m^2 plate area of this condenser is given by

$$Y^* = j\omega\left[\epsilon_0 + \frac{Ne^2/m}{\omega_0^2 - \omega^2 + j2b\omega/m}\right]$$

(c) Consider the circuit in the figure. Show that the admittance of this

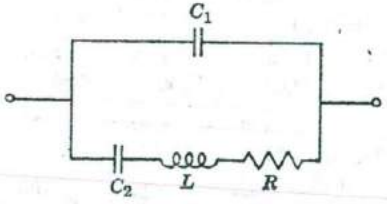

circuit is given by

$$Y^* = jC_1\omega + \frac{j\omega/L}{\omega_0^2 - \omega^2 + jR\omega/L}$$

where $\omega_0^2 = 1/LC_2$.

(d) Compare the results obtained under (b) and (c), and show that the condenser mentioned under (b) has an equivalent circuit as indicated under (c) with the following identifications:

$$C_1 = \epsilon_0; \quad L = m/Ne^2; \quad R = 2b/Ne^2; \quad C_2 = Ne^2/m\omega_0^2$$

3.2 (a) Consider a parallel arrangement of a capacitance C and a resistance R. An external voltage $V(t) = V_0 \cos \omega t$ is applied to this arrangement. Show that the total current $i(t)$ is given by

$$i(t) = (V_0/R) \cos \omega t - C\omega V_0 \sin \omega t$$

(b) Consider a parallel plate condenser with a lossy dielectric between them. At an angular frequency ω let the dielectric be characterized by a complex dielectric constant $\epsilon_r^* = \epsilon_r' - j\epsilon_r''$. The area of the plates is 1 m^2, the distance between them 1 m. For an applied voltage $V(t) = V_0 \cos \omega t$ show that the current through the lossy condenser is given by

$$i(t) = (\epsilon_0\epsilon_r''\omega V_0) \cos \omega t - (\epsilon_0\epsilon_r' V_0\omega) \sin \omega t$$

(c) Compare the results obtained under (a) and (b) and note the occurrence of current components in phase and out of phase with the applied field. Show that the lossy condenser can be represented by an equivalent circuit consisting of a parallel R-C arrangement with

$$R = 1/\epsilon_0\epsilon_r''\omega \qquad \text{and} \qquad C = \epsilon_0\epsilon_r'$$

(d) What is the loss tangent of the condenser in (b) expressed in terms of the equivalent R and C?

(e) Are the elements of the equivalent circuit independent of the frequency?

3.3 (a) Suppose a dielectric has a complex dielectric constant given by $\epsilon_r^* = \epsilon_{ei} + \epsilon_{r0}^*$ where ϵ_{r0}^* refers to the dipole orientations and ϵ_{ei} is a real quantity referring to the electronic and ionic polarizations. Assume that ϵ_{r0}^* is determined by a simple relaxation time τ, as in formula (3.30). Consider the space between two parallel metal plates filled with this dielectric. If the distance between the plates is 1 m, show that the admittance of the condenser per m^2 plate area is equal to

$$Y^* = j\omega\epsilon_0\left[\epsilon_{ei} + 1 + \frac{\epsilon_{r0} - 1}{1 + j\omega\tau}\right]$$

(b) Consider the circuit in the figure. Show that the admittance of this

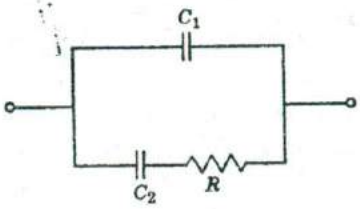

circuit is equal to

$$Y^* = j\omega\left[C_1 + \frac{C_2}{1 + j\omega\tau}\right]$$

where $\tau = RC_2$.

(c) From a comparison of the results obtained under (a) and (b) show that the circuit is the equivalent of the condenser under (a) with the following identification:

$$C_1 = \epsilon_0(\epsilon_{\infty} + 1); \quad C_2 = \epsilon_0(\epsilon_{r0} - 1); \quad R = \tau/[\epsilon_0(\epsilon_{r0} - 1)]$$

3.4 A parallel plate condenser has an area of 10 cm² and a separation of 0.1 mm. The space between the plates is filled with polyethylene. An alternating voltage with an amplitude of 2 volts is applied at a frequency of 1 megacycle. Given that at this frequency the real part of the relative dielectric constant is 2.25 and the loss tangent is 4×10^{-4}, find the elements of an equivalent parallel *R-C* circuit. Also calculate the energy dissipation per second.

3.5 For a polar liquid, make a qualitative sketch of the real and imaginary parts of the dielectric constant at two temperatures as a function of the frequency of an applied radio frequency field.

3.6 For a polar liquid, make a qualitative sketch of the real and imaginary parts of the dielectric constant as a function of temperature at a given radio frequency.

4

Magnetic Properties of Materials

In this chapter we attempt to explain the differences between the various types of magnetic materials in terms of the magnetic properties of atoms and the interactions among these atoms. The chapter is divided into two parts. Part I is intended to refresh the reader's memory on some fundamental concepts concerning magnetic fields, and to illustrate the essence of the atomic theory of magnetic dipoles with reference to simple models. In part II the information gathered in the first part is used to discuss the atomic interpretation of dia-, para-, ferro-, antiferro- and ferrimagnetism.

Part I. Preparatory Discussion

4.1 Summary of concepts pertaining to magnetic fields

In this section the reader is reminded of some fundamental concepts which are discussed in detail in courses on magnetic fields. The *magnetic flux density* in a point of space is denoted by a vector **B**. In the mks system, the unit of flux density may be defined in terms of the force exerted by a magnetic field on a current-carrying wire. Consider, in Fig. 4.1, an element $d\mathbf{l}$ of a wire carrying a current of I amperes; in a magnetic field of flux density **B**, the force on the element $d\mathbf{l}$ is given by

$$d\mathbf{F} = \mathbf{I} \times \mathbf{B}\, d\mathbf{l} \tag{4.1}$$

Thus, the direction of the force $d\mathbf{F}$ is perpendicular to the vectors **I** and **B**, and coincides with the direction in which a right-handed screw advances

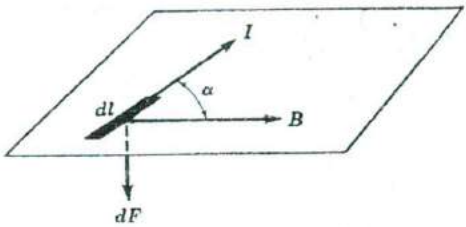

Fig. 4.1. Illustrating the force dF exerted by a magnetic flux density **B** on an element of wire dl carrying a current **I**.

when rotated from **I** to **B**. The magnitude of the force is equal to

$$dF = IB\, dl \sin \alpha \tag{4.2}$$

where α is the angle between **I** and **B** as indicated in Fig. 4.1. Since the proportionality constant in (4.1) has been chosen equal to unity, the units of B are fixed by the units of F (in newtons), I (in amperes), and dl (in meters). Thus, B is expressed in newton $\text{amp}^{-1}\ \text{m}^{-1}$. One usually calls

$$1 \text{ newton amp}^{-1}\ \text{m}^{-1} \equiv 1 \text{ weber m}^{-2} \tag{4.3}$$

Magnetic fields are produced by electric currents; the magnetic flux density produced in a given point by such currents is governed by the law of Biot and Savart. With reference to Fig. 4.2, consider an element dl of

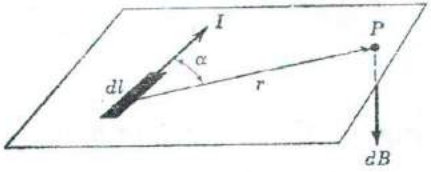

Fig. 4.2. Illustrating the contribution to the flux density, **dB**, resulting from a current-carrying element dl.

a wire carrying a current I as indicated. The flux density contributed by this element in a point P, located at the end of a vector **r** as indicated, is given by

$$d\mathbf{B} = \frac{\mu_0 \mu_r\, dl}{4\pi r^3} \mathbf{I} \times \mathbf{r} \tag{4.4}$$

Here, μ_0 is usually referred to as the *permeability of free space;* it is numerically equal to $4\pi \times 10^{-7} = 1.257 \times 10^{-6}$ henry m^{-1} (or weber $\text{m}^{-1}\ \text{amp}^{-1}$). The quantity μ_r is the *relative permeability* of the medium; it is a pure number which is equal to unity for vacuum. At this point we may remark that μ_0 (as ϵ_0 in the dielectric case) has no physical significance other than that it appears as a result of the particular system of units used here. The

quantity μ_r (as ϵ_r in the dielectric case) is the only parameter which can be interpreted in terms of the *atomic* properties of the medium. According to (4.4), the direction of the flux density $d\mathbf{B}$ is perpendicular to the vectors **I** and **r**, and coincides with the direction in which a right-handed screw advances when rotated from **I** to **r**. The magnitude of the flux density contributed by the element dl in Fig. 4.2 is

$$dB = \frac{\mu_0\mu_r}{4\pi r^2} I\, dl \sin\alpha \tag{4.5}$$

where α is the angle between **I** and **r** as indicated.

As a particular application of the law of Biot and Savart, we leave it up to the reader to show that the magnitude of the flux density produced in a point P by an infinitely long wire carrying a current I is given by

$$B_P = \mu_0\mu_r I/2\pi a \tag{4.6}$$

where a is the distance to point P from the axis of the wire.

In the mks system, the units of the *magnetic field intensity*, **H**, are determined from the notion that the line integral of **H** along a closed curve is equal to the total current enclosed. Thus, with reference to Fig. 4.3 we write

$$\oint \mathbf{H} \cdot d\mathbf{l} = I \tag{4.7}$$

where I represents the current in amperes enclosed by the curve chosen. Thus, the magnetic field intensity H is expressed in amperes m^{-1}. Apply-

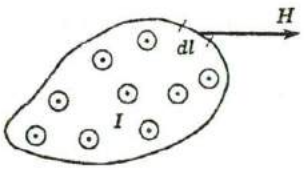

Fig. 4.3. The line integral of **H** along the closed curve is equal to the total current I enclosed by the curve; the current in this case flows into the paper.

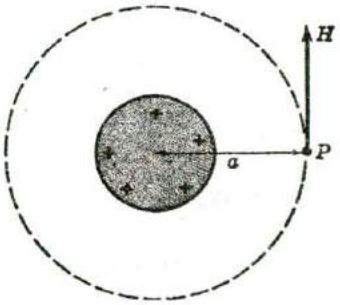

Fig. 4.4. Cross section through a wire carrying a current flowing out of the paper; the magnetic field produced in point P is indicated.

ing this to the case of an infinite wire carrying a current I, let us calculate the magnetic field intensity in a point P at a distance a from the axis of

the wire. Because of the cylindrical symmetry of the problem at hand, we choose as the closed path a circle of radius a (see Fig. 4.4). Then, since **H** is tangent everywhere along the circle, we simply have

$$\oint \mathbf{H} \cdot d\mathbf{l} = 2\pi a H = I$$

or

$$H = I/2\pi a \tag{4.8}$$

Since for the same problem, the flux density is given by (4.6), we arrive at the well-known relation between B and H:

$$\mathbf{B} = \mu_0 \mu_r \mathbf{H} \tag{4.9}$$

In this derivation, we have assumed tacitly that **B** and **H** are parallel vectors; i.e., we have assumed an isotropic medium. We have also assumed that a relative permeability μ_r can be defined for the material in question. This implies that there exists a unique relationship between **B** and **H** in the material, which excludes ferromagnetic materials; the properties of the latter will be discussed in later sections.

4.2 The magnetic dipole moment of a current loop

An essential difference between magnetism and electricity is that in the latter we encounter separate positive and negative charges, whereas in magnetism there are no separate positive and negative poles. This is a consequence of the interpretation of magnetic fields in terms of the motion of electric charges. In the present section we remind the reader of the fact that a current loop produces, at large distances, a magnetic field which is identical with that of a *magnetic dipole moment;* proofs of this statement can be found in textbooks on field theory. In order to illustrate the equivalence of a current loop and a magnetic dipole, we choose an example which is particularly suitable for the subject matter to be discussed in subsequent sections; although we shall consider a simple case, the result is of general validity.

In Fig. 4.5 consider a rectangular wire carrying a current I as indicated; the plane of the rectangle is perpendicular to the paper. We further assume the presence of a homogeneous magnetic flux density **B**, and consider the forces acting on the current-carrying parts of the rectangle. Making use of expression (4.1) one finds for the magnitude of the forces exerted on the elements PS and QR

$$F = (PS)IB \tag{4.10}$$

The directions of the two forces are as indicated in Fig. 4.5. It also follows

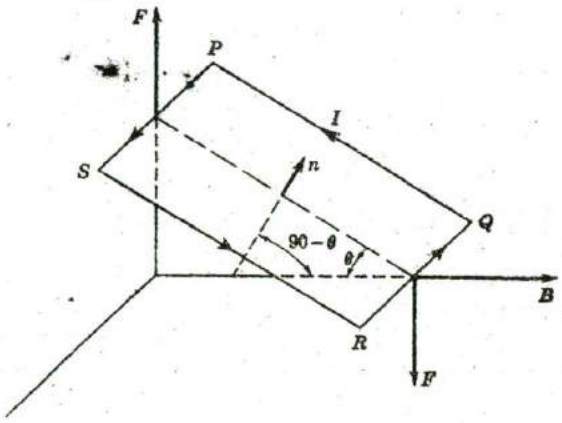

Fig. 4.5. Rectangular current loop $PQRS$, carrying a current I and subjected to a homogeneous flux density **B**. The resultant forces on the rectangle are indicated by F.

from (4.1) that the forces exerted on the elements PQ and RS will cancel each other. Hence, the flux density exerts a torque T on the rectangle, tending to rotate it to the right, equal to

$$IB(PS)(PQ)\cos\theta \tag{4.11}$$

where θ is the angle indicated. Denoting the area of the loop by A, we may write

$$T = IBA\cos\theta \tag{4.12}$$

For later comparison, let **n** denote a unit vector in the direction normal to the rectangle, and pointing upwards, as indicated in Fig. 4.5. The direction of **n** is the same as that in which a right-hand screw would advance when rotated in the direction of the current flow. Since the angle between **n** and **B** is $(90° - \theta)$, we may write

$$\mathbf{T} = IA\mathbf{n} \times \mathbf{B} \tag{4.13}$$

where the magnitude of the cross-product is equal to $B \sin(\mathbf{n}, \mathbf{B}) = B\cos\theta$. At this point, we remind the reader that the torque produced by an electric field **E** on an electric dipole $\boldsymbol{\mu}$ is equal to $\boldsymbol{\mu} \times \mathbf{E}$ (see section 2.5). We thus see that, apart from a constant, expression (4.13) is indistinguishable from that for the torque exerted on a *magnetic dipole moment with its direction along the unit vector* **n**. Although other choices are possible with regard to the units in which one wishes to express magnetic dipole moments, we shall define the magnetic dipole moment $\boldsymbol{\mu}_m$ associated with the current loop as

$$\boldsymbol{\mu}_m = \mathbf{n}IA \tag{4.14}$$

Thus, μ_m is expressed in ampere m^2, and the torque on a magnetic dipole produced by a flux density B is according to (4.14) and (4.13) given by

$$\mathbf{T} = \mu_m \times \mathbf{B} \tag{4.15}$$

Although we have derived the equivalence of a current loop and a magnetic dipole moment for a special geometrical form of the loop, it can be shown that the results apply for a current loop of any shape.

4.3 The magnetization from a macroscopic viewpoint

In the macroscopic description of electric fields, we encountered three vectors: the flux density **D**, the field intensity **E**, and the polarization **P**; the latter represents the electric dipole moment per unit volume in the material. In section 2.2 we derived a relationship between **P** and **E**, leading to the formula

$$\mathbf{P} = \epsilon_0(\epsilon_r - 1)\mathbf{E} \tag{4.16}$$

from which follows, in combination with the formula $\mathbf{D} = \epsilon_0\epsilon_r\mathbf{E}$,

$$\mathbf{D} = \epsilon_0\mathbf{E} + \mathbf{P} \tag{4.17}$$

In the case of magnetic fields one also encounters three vectors: the flux density **B**, the field intensity **H** and the magnetization **M**; the latter is defined as the magnetic dipole moment of the material per m^3. Since we decided in the preceding section to express magnetic dipole moments in ampere m^2, M must have the dimensions of ampere $m^2\ m^{-3}$ = ampere m^{-1}. Hence, M and H have the same dimensions in this system. Note that in the electric case, P has the same dimensions as D rather than as E; the reader should thus consider D and H as corresponding quantities, rather than D and B, in spite of the similar names of the latter two quantities. Although we do not wish to enter here into a detailed discussion concerning the relationship between the electric and magnetic field vectors, we may point out two reasons for the correspondence between D and H, and between E and B. One reason lies in the fact that both E and B are defined from force-laws; E from Coulomb's law between two charges, B from the force exerted by a magnetic field on a current [see (4.1)]. The other reason concerns the definitions of D and H; D is defined from the theorem of Gauss by a surface integral [see (2.1)], and H is defined in terms of a line integral (see (4.7)). Since D and H, and E and B are corresponding quantities, it is not surprising that the formulas encountered in magnetism are *not* analogous to those in dielectrics when considered on the basis of the names of the various quantities; this is somewhat unfortunate, but

one has to live with this situation unless one is willing to introduce a completely new nomenclature.

We shall now proceed to derive a relationship between the macroscopic quantities **B**, **H** and **M**, following the line of thought used in section 2.2 for the derivation of expression (4.16). By comparing that section with the discussion below, the reader will discover the correspondence between D and H, and between B and E mentioned earlier. Consider a solenoid of length L, carrying a current I; the total number of turns is N. The space inside the solenoid is filled with an isotropic homogeneous material of relative permeability μ_r. We shall assume the solenoid to be ideal in the sense that it produces a homogeneous magnetic field in the material (except

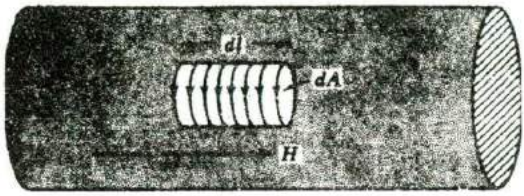

Fig. 4.6. Illustrating a cylindrical piece of material subjected to a homogeneous field **H** produced by a solenoid (not drawn). The lines at the surface of the cylindrical cavity of volume $dl\,dA$ represent the current required to keep the flux density inside the cavity equal to the flux density outside the cavity.

near the ends), as indicated in Fig. 4.6. As shown in textbooks on fields, the magnitude of this field is given by

$$H = NI/L \tag{4.18}$$

This formula also follows from (4.7) by choosing an appropriate path of integration. Note that (4.18) does not contain any parameter characteristic of the material inside the solenoid. The flux density in the material is then in accordance with (4.9) given by

$$B = \mu_0\mu_r NI/L \tag{4.19}$$

Suppose now that we cut out of the material a small cylinder with its axis parallel to the original field direction, as indicated in Fig. 4.6. The cross section of the cylinder will be denoted by dA, its length by dl. How can we achieve a flux density inside the cavity that remains the same as it was when the material was present? Presumably, we are requiring that

$$B_i = B_o = \mu_0\mu_r H \tag{4.20}$$

where the subscript i refers to "inside the cavity" and the subscript o

refers to "outside the cavity." Since inside the cavity we have $\mu_r = 1$, the requirement (4.20) may be written in the form

$$\mu_0 H_i = \mu_0 \mu_r H \quad \text{or} \quad H_i - H = (\mu_r - 1)H \tag{4.21}$$

Hence, in order to leave the flux density inside the cavity the same as the flux density outside, the magnetic field H_i inside the cavity must be larger than that outside by an amount $(\mu_r - 1)H$. This can be achieved by letting a current flow along the inside of the cylindrical surface in the same direction as the current in the solenoid, as indicated in Fig. 4.6. How much current is required to produce the extra field $(\mu_r - 1)H$ inside the cavity? Making use of the physical meaning of (4.18), the answer is evidently $(\mu_r - 1)H\,dl$. However, when this current is allowed to flow, the cavity current corresponds to a magnetic dipole moment equal to

$$\mu_m = (\mu_r - 1)H\,dl\,dA \tag{4.22}$$

Since this current serves the same purpose with regard to a uniform flux density as did the material in the cavity before it was taken out, we conclude that in a homogeneous magnetic field, the material carries a magnetic dipole moment per m^3 equal to

$$\mathbf{M} = (\mu_r - 1)\mathbf{H} = \chi \mathbf{H} \tag{4.23}$$

where $\mathbf{M}$ is called the magnetization. This relation between $\mathbf{M}$ and $\mathbf{H}$ serves the same purpose in the discussion of magnetic materials as does expression (4.16) in the case of dielectrics. Thus, expression (4.23) forms the *link between the macroscopic theory and the atomic interpretation of the permeability* μ_r. The proportionality constant χ is called the *magnetic susceptibility* of the material.

The relationship between $\mathbf{B}$, $\mathbf{H}$, and $\mathbf{M}$ follows immediately from (4.23); multiplying both sides by μ_0, we find

$$\mu_0 \mathbf{M} = \mu_0(\mu_r - 1)\mathbf{H} \quad \text{or} \quad \mathbf{B} = \mu_0(\mathbf{H} + \mathbf{M}) \tag{4.24}$$

The last expression corresponds to (4.17) in the electric case.

4.4 Orbital magnetic dipole moment and angular momentum of two simple atomic models

In the preceding sections we have discussed some important concepts pertaining to the macroscopic theory of magnetism. In the present section we shall consider the magnetic dipole moment and its relation to the angular momentum of two simple atomic models. These models are not correct in the sense that they do not represent our present status of knowledge concerning atoms. However, it is useful to consider the properties

of these classical models because they exhibit the essential features found in the quantum mechanical interpretation of atoms.

(i) Circular Bohr orbit. The first model we shall consider is depicted in Fig. 4.7. It consists of an electron describing a circular orbit of radius R with a stationary nucleus at the center. The charges of the nucleus and

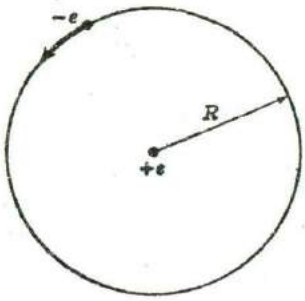

Fig. 4.7. Illustrating an electron describing a circular orbit around a proton. The orbital magnetic dipole moment is directed into the paper.

electron are denoted, respectively, by $+e$ and $-e$. We also assume the electron to rotate with a constant angular velocity of ω radians per second. For the direction of rotation indicated in Fig. 4.7, the motion of the electron in its orbit gives rise to a magnetic dipole moment μ_m directed into the paper and perpendicular to it. The magnitude of the current associated with the electron motion is evidently equal to ef, where $f = \omega/2\pi$ represents the frequency of rotation. Thus, according to (4.14) the magnetic dipole moment of the orbit is

$$|\mu_m| = \pi R^2 e\omega/2\pi = \tfrac{1}{2}e\omega R^2 \tag{4.25}$$

This magnetic dipole moment is called the *orbital magnetic dipole moment*, because it results from the motion of the electron in its orbit around the nucleus. It is of interest to note that there exists a relationship of general validity between the orbital magnetic dipole moment and the *orbital angular momentum*. For the particular case at hand, this relationship may be derived by noting that the angular momentum $\mathbf{M}_a$ is defined as the vector

$$\mathbf{M}_a = \mathbf{R} \times m\mathbf{v} \tag{4.26}$$

where $\mathbf{v}$ is the velocity of the electron and $\mathbf{R}$ the vector which determines its position. Thus, with reference to Fig. 4.7, $\mathbf{M}_a$ is a vector perpendicular to the paper and directed outwardly. Note that $\mathbf{M}_a$ and μ_m have opposite directions; this is a consequence of the negative charge of the electron. Applying (4.26) to the problem under discussion, we find that

$$M_a = m\omega R^2 \tag{4.27}$$

From (4.25) and (4.27) it then follows that

$$\mu_m = -\frac{e}{2m}\,\mathbf{M}_a \tag{4.28}$$

Thus, at least for this particular case, we see that the orbital magnetic moment is equal to $(-e/2m)$ times the angular momentum. We shall see later that (4.28) holds for any charge distribution and so may be considered to have general validity for orbital motion of electrons; it is *not* valid for the electron spin or for the nuclear spin, as we shall see in subsequent sections.

From the quantum theory of atoms it follows that the angular momentum of an electron orbit can most conveniently be expressed in units of $h/2\pi$, where h is Planck's constant [$h = 6.62 \times 10^{-34}$ joule sec; note that according to (4.26), M_a has the same dimensions as h]. For that reason, one has introduced as an atomic unit of magnetic moment the so-called *Bohr magneton*, defined as

$$1 \text{ Bohr magneton} = \frac{e}{2m}\frac{h}{2\pi} = \frac{eh}{4\pi m}$$
$$= 9.27 \times 10^{-24} \text{ ampere m}^2 \tag{4.29}$$

Since the orbital angular momentum of electrons is of the order of $h/2\pi$, the orbital magnetic moment of an electron in an atom is of the order of 1 Bohr magneton.

(ii) **A spherical charge cloud.** As a second example let us consider an atomic model similar to the one used in section 2.3 in the discussion of the

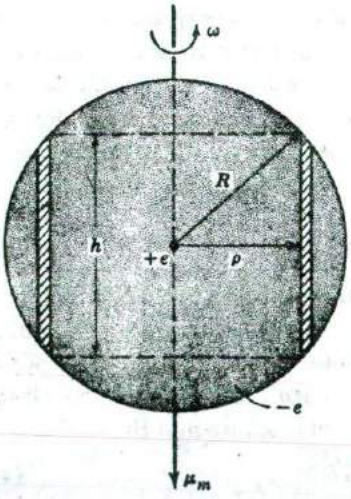

Fig. 4.8. Illustrating the calculation of the magnetic dipole moment μ_m associated with the rotational motion of a charge $-e$ distributed homogeneously throughout a sphere of radius R.

polarizability of an atom. In Fig. 4.8 consider a point charge $+e$ surrounded by a negative charge $-e$, the latter being distributed homogeneously throughout a sphere of radius R. Assuming that the negative charge cloud rotates with a constant angular frequency ω around an axis passing through the center of the sphere, what is the magnetic moment of the system? In view of the axial symmetry of the problem we first consider the contribution to the magnetic moment from the charge moving in the cylindrical shell between ρ and $\rho + d\rho$ indicated in Fig. 4.8. The height of this cylinder is evidently equal to

$$h = 2(R^2 - \rho^2)^{1/2} \tag{4.30}$$

The current associated with this shell, i.e. the charge passing per second through a cross section $h\,d\rho$, is equal to

$$di = q\omega\rho h\,d\rho \tag{4.31}$$

where

$$q = -\frac{e}{(4\pi/3)R^3} \tag{4.32}$$

represents the charge density in the cloud. Thus, the contribution to the magnetic dipole moment is

$$d\mu_m = \pi\rho^2\,di = \pi q h\omega\rho^3\,d\rho \tag{4.33}$$

Hence, the total magnetic moment of the system is given by

$$\mu_m = \pi\omega\int_{\rho=0}^{\rho=R} q h\rho^3\,d\rho \tag{4.34}$$

substituting q and h from (4.30) and (4.32), and carrying out the integration one finds

$$\mu_m = -\tfrac{1}{5}eR^2\omega \tag{4.35}$$

The minus sign means that for the configuration given in Fig. 4.8, μ_m points downwards, as indicated. Comparing the results (4.25) and (4.35) for the two quite different models, it is noted that in both cases the magnitude of the magnetic moment is determined by $e\omega R^2$, and that the results differ only with regard to the numerical constant.

Let us now return for a moment to the expression (4.33), which represents the contribution to μ_m from the cylindrical shell between ρ and $(\rho + d\rho)$. What is the angular momentum associated with the charge moving in this shell? Applying (4.26) we readily find

$$dM_a = \left[\frac{m}{(4\pi/3)R^3}\,2\pi\rho\,h\,d\rho\right]\omega\rho\cdot\rho \tag{4.36}$$

where the term in square brackets represents the mass of the charge between ρ and $(\rho + d\rho)$; we have assumed here that the mass is distributed

homogeneously because we had assumed a homogeneous charge distribution. From (4.33) and (4.36), making use of (4.32), it thus follows that

$$d\mu_m = -\frac{e}{2m}\, d\mathbf{M}_a \tag{4.37}$$

This result is identical with that obtained for the circular orbit discussed under (I). Note that the variable ρ does not occur in (4.37) and that the relationship between $d\mu_m$ and $d\mathbf{M}_a$ holds for any volume element of the charge distribution.

4.5 Lenz's law and induced dipole moments

In this section we shall pursue the properties of the models discussed in the preceding section somewhat further by investigating the influence of a magnetic field on their behavior. Before doing so, the reader is reminded of the well-known law of Lenz. Thus, in Fig. 4.9(a) consider a loop of wire subjected to a magnetic flux which varies with time. Let ϕ be the total flux enclosed by the loop at some instant t. Then, if $d\phi/dt$ is not equal to zero, an electric field is set up in the wire, giving rise to an induced current with a direction such that the magnetic field produced by the current counteracts the $d\phi/dt$. Expressed mathematically, this law takes the form

$$\oint \mathbf{E} \cdot d\mathbf{l} = -d\phi/dt \tag{4.38}$$

The line-integral of the electric field along a closed curve is equal to minus the rate of change of the flux enclosed by the curve; the minus sign indicates that the current produced by the electric field counteracts $d\phi/dt$. This law may be applied to any region of space; i.e., the wire loop mentioned only serves the purpose of detecting the existence of an electric field.

It is of interest to realize the difference in behavior between a wire loop and the atomic models to be discussed below with regard to the effect of a varying magnetic flux. Assume, for example, that the flux enclosed by the wire loop varies with time as indicated in Fig. 4.9(b). For $t = 0$, $\phi = 0$; the flux then increases linearly with time until the constant value ϕ_0 is reached for $t = t_0$. How does the induced current vary with time in this case? According to circuit theory, we may write

$$L\frac{di}{dt} + Ri = -\frac{d\phi}{dt} \tag{4.39}$$

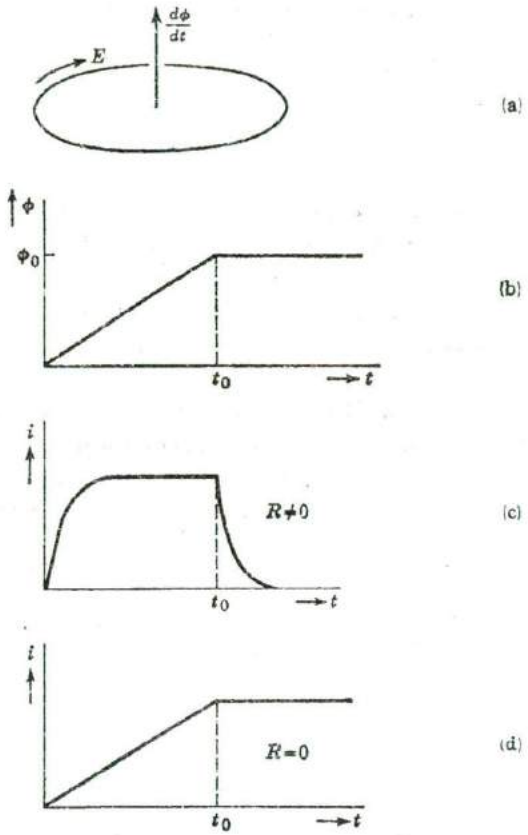

Fig. 4.9. The direction of the electric field produced in a wire loop as a result of a change in the enclosed flux is indicated in (a). (b) represents an assumed $\phi(t)$ relationship. (c) and (d) represent the current induced in the wire loop, respectively, for non-zero resistance and for zero resistance.

where L is the self inductance and R the resistance of the loop. In our case, $d\phi/dt$ is constant for the period between 0 and t_0, and zero for the period $t > t_0$. The solution of equation (4.39), assuming $t_0 \gg L/R$, will look as indicated schematically in Fig. 4.9(c) for the loop with resistance. Thus, the induced current drops to zero after t_0 because there is no longer an electric field. The atomic models to be discussed below are found to behave quite differently. The reason is, that the *electrons in an atom suffer no resistance*, whereas the conduction electrons in a metal wire do. The point we want to make here is that *the atomic models behave as a wire loop*

with zero resistance. In fact, if R is zero, (4.39) reduces to

$$L\frac{di}{dt} = -\frac{d\phi}{dt} \tag{4.40}$$

so that for the $\phi(t)$ given in Fig. 4.9(b), a wire without resistance would carry an induced current $i = \phi/L$ as indicated in Fig. 4.9(d). Note that in this case the current remains constant for $t > t_0$. Thus, a permanent change has been accomplished; the current can be made equal to zero only by reducing the flux ϕ to zero. We shall now proceed to discuss the influence of a varying magnetic flux on the two atomic models of the preceding section.

(i) **Circular Bohr orbit.** Suppose in the absence of a magnetic field an electron of charge $-e$ describes a circle around a nucleus of charge $+e$; let R be the radius of the orbit, and ω_0 the angular frequency. The orbital magnetic dipole moment in the absence of a field is according to (4.25) equal to

$$\mu_m = -\tfrac{1}{2}eR^2\omega_0 \tag{4.41}$$

Suppose now that the magnetic flux density is increased from zero to some value B, where B is directed into the paper in Fig. 4.10. Assuming for

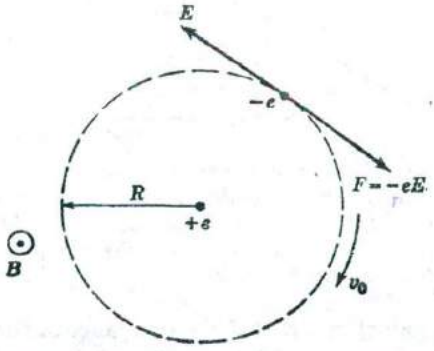

Fig. 4.10. The electron describes a circular orbit around a proton with an initial velocity v_0 as indicated. A magnetic field of flux density B into the paper is applied. The electric field E and the force F resulting from the change in magnetic flux are indicated.

simplicity that the radius of the orbit remains constant, the electron will experience an electric field E, tangential to the orbit everywhere, equal to

$$E = -\frac{1}{2\pi R}\frac{d\phi}{dt} = -\frac{R}{2}\frac{dB}{dt} \tag{4.42}$$

This follows immediately by applying (4.38) to the present case. The

force on the electron during the period that **B** changes with time is then equal to

$$F = -eE = \frac{eR}{2}\frac{dB}{dt} \tag{4.43}$$

The direction of the force **F** for the configuration in Fig. 4.10 is indicated; it is observed that this force tends to accelerate the electron. Now, according to classical mechanics, a force acting during a period dt changes the momentum of a particle in accordance with the equation

$$F\,dt = d(mv) = m\,dv \tag{4.44}$$

where v is the velocity of the particle. In our case, let $\omega(t)$ be the angular frequency of the electron in its orbit at the instant t. It then follows from (4.43) and (4.44) that

$$\frac{eR}{2}\frac{dB}{dt}\,dt = mR\,d\omega \quad \text{or} \quad d\omega = \frac{e}{2m}\,dB \tag{4.45}$$

Assuming that for $B = 0$ the angular frequency is ω_0, we find that for any value B the angular velocity is given by

$$\omega = \omega_0 + \frac{e}{2m}\mathbf{B} \equiv \omega_0 + \omega_L \tag{4.46}$$

where ω_L is called the *Larmor angular frequency*. Since the angular frequency of the electron has changed upon application of the magnetic field, *the orbital magnetic dipole moment has also changed*. In fact, before the field was applied the orbital magnetic moment was

$$\mu_{m0} = -\tfrac{1}{2}eR^2\omega_0$$

and after the field has been applied it is

$$\mu_m = -\frac{1}{2}eR^2\omega_0 - \frac{e^2}{4m}R^2\mathbf{B}$$

The magnetic dipole moment induced by the field is therefore

$$\mu_{m\,\mathrm{ind}} = \mu_m - \mu_{m0} = -\frac{e^2}{4m}R^2\mathbf{B} \tag{4.47}$$

Note that the *induced dipole moment has a direction opposite to the applied magnetic field*, in contrast with the electric dipole moment induced by an electric field (see section 2.3); this result is independent of the initial direction of rotation, as the reader may verify for himself. Also note that since the electron suffers no resistance, it will keep its new angular frequency ω as long as B remains constant; it thus behaves as the wire loop of zero resistance discussed at the beginning of this section.

An alternative derivation of (4.46) and (4.47) may be given in the

following manner: With reference to Fig. 4.11, consider an electron moving in a circular orbit of radius R around the nucleus. In the presence of a magnetic field of flux density B, the stability of the orbit requires equilibrium between three forces: (a) the centrifugal force mv^2/R; (b) the

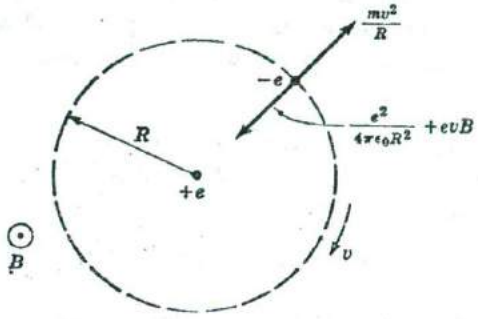

Fig. 4.11. Illustrating the equilibrium condition for a circular orbit described by an electron around a proton in the presence of a magnetic field of flux density B into the paper.

Coulomb force $e^2/4\pi\epsilon_0 R^2$ due to attraction by the nucleus; (c) the "Lorentz force" $-e\mathbf{v} \times \mathbf{B}$ due to the magnetic field. For the configuration in Fig. 4.11 we thus require

$$\frac{mv^2}{R} = \frac{1}{4\pi\epsilon_0}\frac{e^2}{R^2} + evB$$

or

$$\omega^2 = \frac{1}{4\pi\epsilon_0}\frac{e^2}{mR^3} + \frac{eB}{m}\omega \tag{4.48}$$

In the absence of a magnetic field, let the angular frequency of rotation be ω_0; then according to (4.48) we obtain by putting $B = 0$

$$\omega_0^2 = \frac{1}{4\pi\epsilon_0}\frac{e^2}{mR^3} \tag{4.49}$$

In the presence of a magnetic field we may therefore write (4.48) in the form

$$\omega^2 = \omega_0^2 + \frac{eB}{m}\omega \tag{4.50}$$

Now, $\omega_0 \cong 10^{15}$ radians per second for the motion of an electron in an atom (see section 3.1). Since the magnetic fields used in the laboratory are of the order of $B \cong 1$ weber m^{-2} or less, we see that $eB/m \cong 10^{11}$ per second which is much smaller than ω_0. Making use of this, one finds readily by

solving for ω from (4.50)

$$\omega \cong \omega_0 + \frac{e}{2m} B \tag{4.51}$$

which is the same as (4.46). The reader may be somewhat astonished by the fact that (4.51) is an approximation whereas it looks as if (4.46) is exact. This is only an apparent contradiction and is a result of the fact that in both derivations we have assumed R to be independent of B, which is itself an approximation, valid only as long as $eB/m \ll \omega_0$.

(ii) **Homogeneous spherical charge distribution.** Let us now consider the model consisting of a charge $-e$ distributed homogeneously throughout a sphere of radius R; a point charge $+e$ is located at the center of the

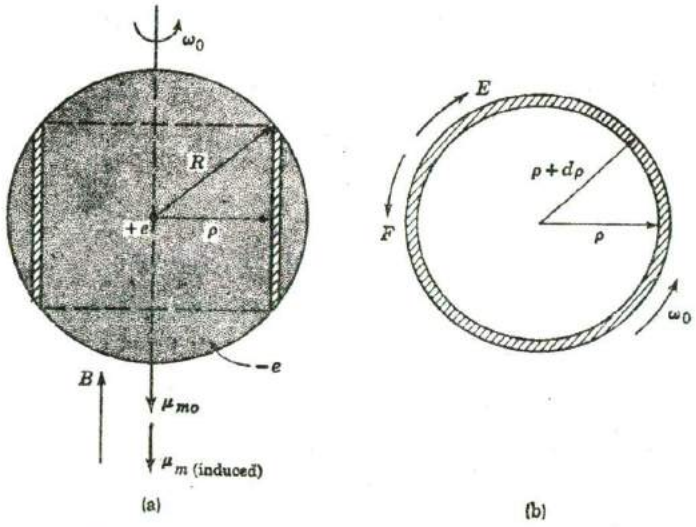

Fig. 4.12. Illustrating the geometry pertaining to the calculation of the magnetic dipole moment induced by a homogeneous flux density B in a spherical charge cloud $-e$. In (b) a top view is given, illustrating the cylindrical shell of charge between ρ and $\rho + d\rho$, the electric field E and the force F exerted on the shell of charge.

sphere so as to make the "atom" neutral. In the absence of a magnetic field, let the negative charge cloud rotate around a vertical axis, passing through the center of the sphere, with an angular frequency ω_0 as indicated in Fig. 4.12(a). The magnetic dipole moment of the system is then directed

downwards in Fig. 4.12(a), and is given by

$$\mu_{m0} = -\tfrac{1}{5}eR^2\omega_0 \tag{4.52}$$

[see equation (4.35)].

Let us now apply a magnetic field of flux density B, where B is directed vertically upwards in Fig. 4.12(a). In order to calculate the induced moment in this case we proceed as follows. As in the preceding section, consider the charge rotating in a cylindrical shell between ρ and $\rho + d\rho$ of height $h = 2(R^2 - \rho^2)^{1/2}$. As long as the flux changes, the electric field produced at a distance ρ from the axis is obtained by applying (4.38), giving

$$E = -\frac{1}{2\pi\rho}\frac{d\phi}{dt} = -\frac{\rho}{2}\frac{dB}{dt} \tag{4.53}$$

The field E is tangential to the circle of radius ρ and has a direction as indicated in Fig. 4.12(b). The force exerted by this field on the negative charge thus tends to increase the angular frequency for the configuration assumed in Fig. 4.12(b). The charge in the cylindrical shell divided by the mass in the cylindrical shell is simply equal to $-e/m$, assuming that both charge and mass are distributed homogeneously. From Newton's law (4.44) it thus follows that

$$-\frac{e}{m}E\,dt = \rho\,d\omega \tag{4.54}$$

and since $E(\rho)$ is given by (4.53) we find

$$d\omega = \frac{e}{2m}d\mathbf{B} \tag{4.55}$$

Since this result is independent of ρ, it holds for the whole sphere of charge. Therefore, if for $B = 0$ the angular frequency is equal to ω_0, we find that for any flux density B the angular frequency is given by

$$\omega = \omega_0 + \frac{e}{2m}\mathbf{B} \equiv \omega_0 + \omega_L \tag{4.56}$$

This result is identical with (4.46) and it will be evident to the reader that the Larmor frequency induced by the magnetic field is independent of the particular charge distribution assumed. The magnitude of the induced dipole moment, of course, does depend on the model. In fact, from (4.35) and (4.56) it follows that for the model under discussion

$$\mu_{m\,\mathrm{ind}} = -\frac{e^2}{10m}R^2\mathbf{B} \tag{4.57}$$

which differs from (4.47) for a circular orbit by a numerical factor. In the

derivation given we have assumed tacitly that the charge distribution is independent of the flux density of the applied magnetic field; for practical flux densities obtainable in the laboratory this assumption is justified.

Note that the induced moment is independent of the initial angular frequency ω_0 of the charge distribution. Hence, a magnetic dipole moment given by (4.57) will be induced in the atomic model, independent of whether the model has a "permanent" magnetic dipole moment or not.

Part II. Atomic Interpretation of Magnetic Properties of Materials

4.6 Classification of magnetic materials

In this part of the chapter we shall discuss the most essential features of the various types of magnetic materials in terms of the magnetic properties of the atomic dipoles and the interactions between them. The first distinction we can make is that between materials whose atoms carry *permanent magnetic dipoles* and those in which permanent magnetic dipoles are absent; the term permanent magnetic dipole is used here in the same sense as in the corresponding dielectric case; i.e., a permanent dipole exists even in the absence of a field. Materials which lack permanent magnetic dipoles are called *diamagnetic*. If there are permanent magnetic dipoles associated with the atoms in a material, such a material may be *paramagnetic*, *ferromagnetic*, *antiferromagnetic*, or *ferrimagnetic*, depending on the interaction between the individual dipoles. Thus, if the interaction between the atomic permanent dipole moments is zero or negligible, a material will be paramagnetic. If the dipoles interact in such a manner that they tend to line up in parallel, the material will be ferromagnetic. If neighboring dipoles tend to line up so that they are antiparallel, the material is antiferromagnetic or ferrimagnetic, depending on the magnitudes of the dipoles on the two "sub lattices," as indicated schematically for a one-dimensional model in Fig. 4.13. Note that in the ferromagnetic case, there is a large resultant magnetization, whereas in an antiferromagnetic configuration the magnetization vanishes. In the case of ferrimagnetic materials, there may be a relatively large net magnetization resulting from the tendency of antiparallel alignment of neighboring dipole moments of unequal magnitude. Ferrimagnetic materials are thus similar to ferromagnetic ones in the sense that both kinds may exhibit a large magnetization. On the other hand, ferrimagnetic materials resemble antiferromag-

netic materials with respect to the tendency for antiparallel alignment of neighboring dipole moments.

We should add here a remark to the effect that *induced dipole moments occur in all materials.* In fact, in section 4.5 we showed that a dipole moment induced by a magnetic field in a particular atomic model was inde-

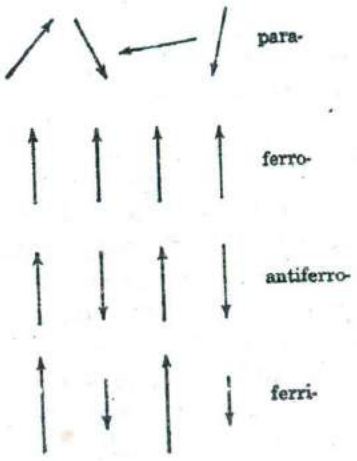

Fig. 4.13. Schematic illustration of a paramagnetic, ferromagnetic, antiferromagnetic, and ferrimagnetic arrangement of spins.

pendent of the magnetic dipole moment present in the absence of the field. In this sense then, all materials are diamagnetic. However, when permanent dipole moments are present in numbers comparable to the total number of atoms, the properties of the permanent dipoles usually overshadow the diamagnetic effects and for that reason the classification given above is meaningful.

In the present section we only wish to introduce the classification of magnetic materials; the actual properties of the various kinds of magnetic materials will be discussed in subsequent sections. A summary of the definitions of the various classes of magnetic materials is given in Table 4.1.

Table 4.1. CLASSIFICATION OF MAGNETIC MATERIALS ON THE BASIS OF THE OCCURRENCE OF PERMANENT ATOMIC MAGNETIC DIPOLES, AND THE INTERACTION BETWEEN THEM

Classification	Permanent dipoles	Interaction between neighboring dipoles
Diamagnetic	No	———
Paramagnetic	Yes	Negligible
Ferromagnetic	Yes	Parallel orientation
Antiferromagnetic	Yes	Antiparallel orientation of equal moments
Ferrimagnetic	Yes	Antiparallel orientation of unequal moments

4.7 Diamagnetism

The link between the macroscopic and atomic interpretation of magnetism is provided by the formula for the magnetic dipole moment per unit volume, derived in section 4.3,

$$M = (\mu_r - 1)H = \chi H \tag{4.58}$$

It was stated in that section that (4.58) has meaning only if one can define the relative permeability μ_r for the material under discussion; thus (4.58) is valid for diamagnetic and paramagnetic materials at all temperatures, but for the other classes only above a certain temperature, as we shall see in later sections. The permeability μ_r, or the susceptibility χ for a diamagnetic or paramagnetic specimen can be determined, for example, by measuring the force exerted on a specimen in an inhomogeneous field (Gouy balance). In Table 4.2 we have given the susceptibility for some

Table 4.2. THE SUSCEPTIBILITY OF SOME DIAMAGNETIC MATERIALS (AT ROOM TEMPERATURE)

Material	$\chi = \mu_r - 1$	Material	$\chi = \mu_r - 1$
Al_2O_3	-0.5×10^{-5}	Cu	-0.9×10^{-5}
$BaCl_2$	-2.0×10^{-5}	Au	-3.6×10^{-5}
NaCl	-1.2×10^{-5}	Ge	-0.8×10^{-5}
Diamond	-2.1×10^{-5}	Si	-0.3×10^{-5}
Graphite	-12×10^{-5}	Se	-1.7×10^{-5}

diamagnetic materials. We should note that in the case of metals and semiconductors the susceptibility contains a small paramagnetic contribution associated with the spins of the conduction electrons (the electron spin will be taken up in the next section). It is observed that for these diamagnetic materials the permeability is given approximately by

$$\mu_r \cong 1 - 10^{-5}$$

As long as the electronic structure of the material is independent of temperature, the diamagnetic susceptibility is also essentially independent of temperature. For most engineering applications, μ_r of a diamagnetic material may be taken as equal to unity.

It is of interest to investigate to what extent the theory of section 4.5 is in agreement with the observed values. From the discussion in section 4.5 it will be evident that an actual calculation of the induced dipole moment would require a detailed knowledge of the electronic structure of the atom. However, an estimate of the order of magnitude of the diamagnetic

properties may be obtained by making use of expression (4.57). Assuming that an atom contains, say, 10 electrons, we estimate from (4.57) that the induced magnetic moment should be of the order of

$$\mu_{m\,\text{ind}} \approx -\frac{e^2}{m} R^2 B = -\frac{e^2}{m} R^2 \mu_0 \mu_r H$$

Taking $R \approx 10^{-10}$ m and assuming $N \cong 5 \times 10^{28}$ atoms per m^3, we find from $M = N\mu_{m\,\text{ind}} = \chi H$ a value for χ of the order of 10^{-6}, in agreement with the experimental values quoted in Table 4.2. There thus seems little doubt that the interpretation of diamagnetism in terms of Lenz's law acting on an atomic scale is essentially correct.

4.8 The origin of permanent magnetic dipoles in matter

According to the classification given in section 4.6, the properties of paramagnetic, ferromagnetic, antiferromagnetic, and ferrimagnetic materials are determined by the presence of permanent magnetic dipoles. In this section we shall discuss the various contributions to the permanent magnetic dipole moment of the atomic constituents of matter. According to the results obtained in section 4.4 we can say that whenever a charged particle has an angular momentum, the particle will contribute to the permanent dipole moment. In general, there are three contributions to the angular momentum of an atom:

(i) *orbital angular momentum of the electrons,*
(ii) *electron spin angular momentum,*
(iii) *nuclear spin angular momentum.*

Each of these forms of angular momentum corresponds to a permanent magnetic dipole moment and the total magnetic dipole moment of an atom is obtained by adding the components in an appropriate manner. The rules governing the addition of these components are derived from quantum mechanics and will not be discussed in this book, except in some simple cases. We shall now discuss the contributions separately.

(i) **Orbital magnetic dipole moments.** The relationship between the orbital magnetic dipole moment and the orbital angular momentum has been discussed in terms of a classical model already in section 4.4; we obtained there the relationship [see (4.28)]

$$\boldsymbol{\mu}_m = -\frac{e}{2m} \mathbf{M}_o \qquad (4.28)$$

and this remains valid in the quantum theory. However, quantum theory shows that the orbital angular momentum of an electron in an atom

exhibits certain features which are not exhibited by classical models. In section 1.2 we mentioned that the orbital state of motion of an electron in an atom is described by three quantum numbers n, l and m_l. The *principal quantum number* n determines the energy of the electron; the *orbital quantum number* l determines the orbital angular momentum, and the *magnetic quantum number* m_l determines the component of the angular momentum along an external field direction. The quantum numbers can accept only discrete values, and the rules pertaining to these values as derived from quantum mechanics are the following:

$$\begin{aligned} n &= 1, 2, 3, \ldots \\ l &= 0, 1, \ldots, (n-1) \\ m_l &= l, (l-1), \ldots, 0, -1, \ldots, -l \end{aligned} \tag{4.59}$$

The physical meaning of the magnetic quantum number m_l can be understood within the framework of our present discussion from the following considerations. In atomic physics, angular momentum is measured in units of $h/2\pi$, where h ($= 6.62 \times 10^{-34}$ joule sec) represents Planck's constant. Thus, an electron for which $l = 0$ has no angular momentum and as a consequence of (4.28) also no orbital magnetic dipole moment. An electron for which $l = 1$ can orient itself in such a manner in an applied magnetic field that the components of the angular momentum along the field direction are given by the possible values of m_l as follows:

$$(h/2\pi), \quad 0, \quad -(h/2\pi)$$

These components correspond to the m_l values 1, 0, -1, dictated by (4.59). Hence, for $l = 1$, the possible components of the orbital magnetic dipole moment are given by [see (4.28)]

$$-(eh/4\pi m), \quad 0, \quad +(eh/4\pi m) \tag{4.60}$$

as indicated schematically in Fig. 4.14. The reader is reminded here of equation (4.29), which defines the frequently encountered quantity $eh/4\pi m$ as 1 Bohr magneton. In general then, the component of the orbital

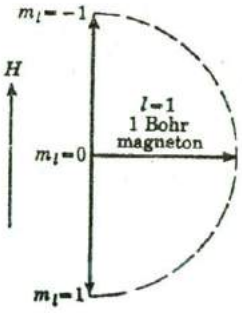

Fig. 4.14. Illustrating the three possible components of the magnetic dipole moment in an external field H, associated with an orbital momentum quantum number $l = 1$. The total angular momentum is actually equal to $(h/2\pi)\sqrt{l(l+1)}$, and in this sense the figure is somewhat misleading.

magnetic dipole moment along an external field is equal to $-m_l$ Bohr magnetons. From the theory of the periodic table, discussed in Chapter 1, and from the remarks just made, one can readily show that a completely filled electronic shell contributes nothing to the orbital permanent dipole moment of an atom. Consider, for example, the *L*-shell, corresponding to $n = 2$. The possible l-values are then 0 and 1. For $l = 0$ there is no magnetic dipole moment anyway. For $l = 1$ we have $m_l = 1, 0, -1$ and if these states are all occupied, the sum of their components vanishes according to (4.60). In general then, one can only expect a resultant orbital magnetic moment in atoms containing incompletely filled electronic shells, and even then the resultant may be zero. Of particular interest to the physicist in this respect are the transition elements; i.e., those elements which have incompletely filled inner shells. A look at Table 1.1, giving the electron configurations of a number of atoms, shows that the elements 21 through 28 (the iron group) fall in this category. Similarly, elements 39 through 45, 58 through 71 (the rare earths) and 89 through 92 are transition elements. For the electrical engineer, the elements of the iron group are of greatest importance. However, in the solid state the orbital magnetic moments of these elements or their compounds are "frozen in." Thus, although the free atoms do have a resultant orbital magnetic moment, the contribution of these moments to the magnetic properties in the solid state is negligible. The reason is that in the iron group the incompletely filled shell lies near the outside of the atoms and is thus highly susceptible to interaction with neighboring atoms in the lattice. As a result of this interaction the dipole moments cannot orient themselves in an external field. In this respect they behave in a way similar to the immobile permanent electric dipole moments in a solid (see Section 2.7).

We should remark here, that for the elements of the rare earths group, the permanent orbital dipole moments do contribute to the magnetic susceptibility. In these elements, the incomplete shells lie relatively deep inside the atom, so that they interact with neighboring atoms to a much smaller degree than do the iron group elements.

In subsequent sections, the contribution from the orbital magnetic dipoles will be neglected, but the reader should realize that this is not always permissible.

(ii) **Electron spin magnetic moment.** In order to explain the details of atomic spectra, Uhlenbeck and Goudmit in 1925 introduced the hypothesis that the electron itself has an angular momentum; i.e., an angular momentum over and above that corresponding to its orbital motion in an atom. The angular momentum of the electron itself is referred to as the

spin of the electron. Since the electron has a charge, the spin produces a magnetic dipole moment. According to quantum theory, the spin angular momentum along a given direction is either $+h/4\pi$ or $-h/4\pi$; i.e., it can accept only two possible orientations in an external magnetic field. The relationship between the spin angular momentum and the spin magnetic dipole moment is given by

$$\mu_{m\,\text{spin}} = -\frac{e}{m}\,\mathbf{M}_{a\,\text{spin}} \tag{4.61}$$

which differs from (4.28) by a factor of 2 on the right-hand side. Thus, the relationship between angular momentum and magnetic dipole moment for the electron spin cannot be understood in terms of a simple classical picture of a rotating sphere of charge. As a result of (4.61) the spin dipole moment components along an external field are

$$+\frac{e}{m}\frac{h}{4\pi} = +1 \text{ Bohr magneton or } -\frac{e}{m}\frac{h}{4\pi} = -1 \text{ Bohr magneton} \tag{4.62}$$

as indicated in Fig. 4.15. In a many-electron atom, the individual spin magnetic moments are added in accordance with certain rules. Here, as in the case of orbital moments, completely filled shells contribute nothing

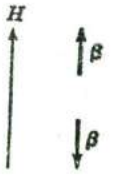

Fig. 4.15. Illustrating the two possible moment components associated with the electron spin in an external field H; β represents 1 Bohr magneton.

to the resultant spin moment. However, an atom such as Na, with one valence electron, has a resultant dipole moment equal to that produced by the valence electron. A sodium ion, Na^+, on the other hand, has no resultant spin moment, because the electronic shells are completely occupied. For engineering applications the atoms or ions of the iron group elements are of greatest interest. In Table 4.3 we give the spin configuration associated with the electrons in the incompletely filled 3*d*-shell ($n = 3$, $l = 2$) for these elements. The configurations apply to the free atoms as well as to the divalent ions of these elements. In the metallic state, the situation is more complicated and Table 4.3 does not apply. For example, in metallic iron, the average number of Bohr magnetons per atom is 2.2 rather than 4 for the free atom or the Fe^{2+} ion; the non-integral number of Bohr magnetons per atom in the metallic state can be explained in terms of the energy band structure of the transition metals.

Table 4.3. NUMBER OF ELECTRONS IN THE $3d$-STATE ($n = 3$, $l = 2$) AND ALIGNMENT OF INDIVIDUAL SPINS FOR THE FREE ATOMS OR DIVALENT IONS OF THE IRON GROUP ELEMENTS; CALCIUM AND COPPER HAVE BEEN ADDED FOR COMPARISON

Atomic number	Element	$3d$	Resultant spin in Bohr magnetons
20	Calcium	0	0
21	Scandium	1	1 ↑
22	Titanium	2	2 ↑ ↑
23	Vanadium	3	3 ↑ ↑ ↑
24	Chromium	4	4 ↑ ↑ ↑ ↑
25	Manganese	5	5 ↑ ↑ ↑ ↑ ↑
26	Iron	6	4 ↑ ↑ ↑ ↑ ↑ ↓
27	Cobalt	7	3 ↑ ↑ ↑ ↑ ↑ ↓ ↓
28	Nickel	8	2 ↑ ↑ ↑ ↑ ↑ ↓ ↓ ↓
29	Copper	10	0 ↑ ↑ ↑ ↑ ↑ ↓ ↓ ↓ ↓ ↓

(iii) **Nuclear magnetic moments.** The angular momentum associated with the nuclear spin is measured in units $h/2\pi$, and is of the same order of magnitude as the electron spin and the orbital angular momentum of the electrons. However, the mass of the nucleus is larger than that of an electron by a factor of the order of 10^3. Consequently, the magnetic dipole moment associated with the nuclear spin is of the order of 10^{-3} Bohr magnetons. Since the nuclear dipole moments are small compared to those associated with the electrons, we may neglect the influence of the former on the magnetic properties of the materials of interest in this book.

In summary then, we shall consider in the following sections only the properties of the electron spin system, assuming that neither the orbital magnetic moments nor the nuclear magnetic moments contribute to the properties of the materials. It should be kept in mind that these omissions are imposed by the limited scope of this book, and that the physicist may be interested, for example, in studying the properties of the nuclear spin system.

4.9 Paramagnetic spin systems

In this section we shall consider the susceptibility of a material in as far as it is determined by the presence of electron spin magnetic dipole moments. For simplicity, we shall deal only with a system of spins of one Bohr magneton (such as the scandium atom in Table 4.3); in that case an individual dipole can accept only two possible components along an

applied field direction, viz. +1 or −1 Bohr magneton. For atoms with larger spin moments, the calculations are somewhat more complicated, but the essential features are the same. In the present section we shall assume that the interaction between the spins is negligible, so that the field at the position of a given spin may be taken equal to the applied field H. This also implies that the flux density at the position of a given spin is assumed to be $B = \mu_0 H$. In making this assumption, we confine ourselves in this section to paramagnetic materials (see the classification in Table 4.1).

Let there be N spins per m³ in the material. In the absence of an applied field, there are as many "up" spins as "down" spins, so that the magnetization $M = 0$. In a field H, there will be a preference for the dipoles to line up parallel to the field, and some magnetization will result. At a temperature T, let there be N_p dipoles per m³ parallel to the field, and N_a antiparallel; we must then require

$$N_p + N_a = N \tag{4.63}$$

For convenience we shall denote a Bohr magneton by β, where $\beta = eh/4\pi m$. The magnetization is then given by

$$M = (N_p - N_a)\beta \tag{4.64}$$

Since the macroscopic susceptibility is given by

$$\chi = \mu_r - 1 = M/H \tag{4.65}$$

we wish to express $N_p - N_a$ in terms of H, because we shall then be able to express χ in terms of atomic quantities. As indicated in Fig. 4.16, the

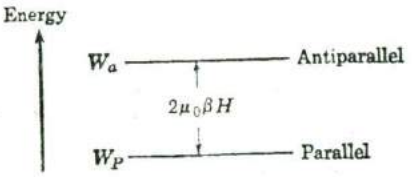

Fig. 4.16. Illustrating the energy difference between spin magnetic dipoles parallel and antiparallel to an external field.

energy of a magnetic dipole in the field with antiparallel orientation is larger than that with parallel orientation. The energy difference can be calculated from the fact that the torque, according to (4.15), is in general given by $\boldsymbol{\mu}_m \times \mathbf{B}$, which in our case reduces to $\mu_0 \boldsymbol{\mu}_m \times \mathbf{H}$. It is left to the reader to show that the energy difference between antiparallel and parallel orientation is given by

$$W_a - W_p = 2\mu_0 \beta H \tag{4.66}$$

According to Boltzmann's statistics then, we have for the ratio N_a/N_p

the expression

$$N_a/N_p = \exp\left[(W_p - W_a)/kT\right]$$
$$= \exp\left(-2\mu_0\beta H/kT\right) \tag{4.67}$$

Thus, we know the sum and the ratio of N_a and N_p. It follows from (4.63) and (4.67) that

$$N_p = \frac{N}{1 + \exp\left(-2\mu_0\beta H/kT\right)} = \frac{N \exp\left(\mu_0\beta H/kT\right)}{\exp\left(\mu_0\beta H/kT\right) + \exp\left(-\mu_0\beta H/kT\right)} \tag{4.68}$$

$$N_a = \frac{N}{1 + \exp\left(2\mu_0\beta H/kT\right)} = \frac{N \exp\left(-\mu_0\beta H/kT\right)}{\exp\left(\mu_0\beta H/kT\right) + \exp\left(-\mu_0\beta H/kT\right)}$$

Substituting these expressions into (4.64) we find for the magnetization

$$M = N\beta \tanh\left(\mu_0\beta H/kT\right) \tag{4.69}$$

In Fig. 4.17 we have plotted $M/N\beta$ as a function of the variable $x = \mu_0\beta H/kT$. Note that for $x \ll 1$, $\tanh(x) \cong x$, and that for $x \gg 1$,

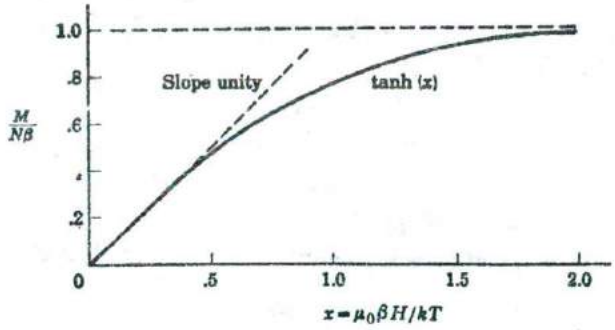

Fig. 4.17. The fully drawn curve represents $M/N\beta$ as a function of $x = \mu_0\beta H/kT$. For $x \ll 1$, $\tanh(x) \cong x$, corresponding to a line through the origin of slope unity.

$\tanh(x)$ approaches unity. Hence, for strong fields and low temperatures, the magnetization approaches $N\beta$; i.e., it approaches the situation in which all dipoles are lined up in parallel with the field. An example of a paramagnetic salt exhibiting *saturation of the magnetization* is given in Fig. 4.18. For normal temperatures and for not too high fields, $\mu_0\beta H \ll kT$ and under those circumstances $x \ll 1$, so that

$$M \cong N\mu_0\beta^2 H/kT \qquad \text{for} \qquad \mu_0\beta H \ll kT \tag{4.70}$$

In practice, the condition $\mu_0\beta H \ll kT$ is satisfied more often than not. For example, even for a relatively strong field $\mu_0 H \approx 1$ weber m^{-2} we have $\mu_0\beta H \approx 9 \times 10^{-24}$ joule, whereas at room temperature $kT \cong 4 \times 10^{-21}$

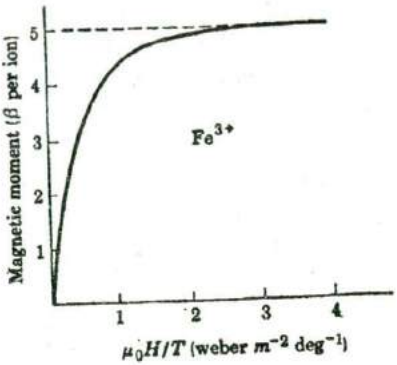

Fig. 4.18. The magnetic moment in Bohr magnetons per Fe^{3+} ion in ferric ammonium alum as a function of $\mu_0 H/T$; note the observed approach to the saturation value of 5β. [After W. E. Henry, *Phys. Rev.* 88, 559 (1952)]

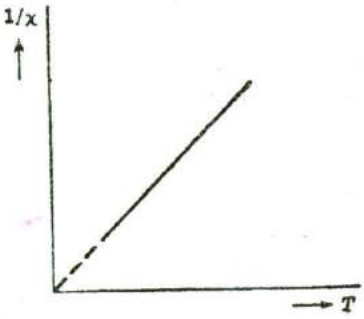

Fig. 4.19. The reciprocal of the susceptibility as a function of T for a paramagnetic material, illustrating the Curie law.

joule. Assuming that (4.70) is valid, we find from (4.65) and (4.70) for the susceptibility

$$\chi = \mu_r - 1 = N\mu_0\beta^2/kT \equiv C/T \tag{4.71}$$

Thus, the susceptibility varies as $1/T$; it is instructive in this connection to compare the similar problem of orientational polarization in dielectrics, discussed in section 2.5. The law expressed by (4.71) is known as the *Curie law* of paramagnetism; it is illustrated in Fig. 4.19. The constant $C = N\mu_0\beta^2/k$ is called the *Curie constant.*

An estimate of the magnitude of χ (or μ_r) at a given temperature may be made by taking $N \cong 5 \times 10^{28}$ m^{-3}. Putting in numerical values for the other quantities in (4.71), one finds $\chi \cong 0.3/T$; i.e., χ is of the order of 10^{-3} at room temperature. Experimentally determined values are given in Table 4.4; it is observed that these are of the estimated order of magni-

Table 4.4. SUSCEPTIBILITIES OF SOME PARAMAGNETIC MATERIALS AT ROOM TEMPERATURE

Substance	$\chi = \mu_r - 1$	Substance	$\chi = \mu_r - 1$
$CrCl_3$	1.5×10^{-3}	Fe_2O_3	1.4×10^{-3}
Cr_2O_3	1.7×10^{-3}	$Fe_2(SO_4)_3$	2.2×10^{-3}
CoO	5.8×10^{-3}	$FeCl_2$	3.7×10^{-3}
$CoSO_4 \cdot H_2O$	2.0×10^{-3}	$FeSO_4$	2.8×10^{-3}
$MnSO_4$	3.6×10^{-3}	$NiSO_4$	1.2×10^{-3}

tude. It should be realized that the measured susceptibility includes a diamagnetic contribution which has not been considered in the present section. However, since susceptibilities are additive quantities, and since $\chi_{dia} \approx 10^{-5}$ according to the results in section 4.7, we see that $\chi_{dia} \ll \chi_{para}$ at room temperature and below.

For many applications in electrical engineering, it is a good approximation to take the relative permeability μ_r of paramagnetic substances equal to unity. As far as applications of paramagnetic materials are concerned, we may mention here that paramagnetic salts are the working material used in obtaining very low temperatures ($< 1°K$) by *adiabatic demagnetization:* the principle of this method is discussed in the books by Kittel and by Dekker, given in the list of general references. Also, paramagnetic salts have entered the group of electrical engineering materials a few years ago because they are the essential material used in the solid state *maser* (microwave amplification through stimulated emission by radiation). The principle of operation of a maser is discussed in van der Ziel's book (page 590 ff), cited in the general references.

4.10 Some properties of ferromagnetic materials

Each ferromagnetic material has a characteristic temperature above which its properties are quite different from those below that temperature. This temperature is called the *ferromagnetic Curie temperature* and will be denoted here by θ_f. In this section we shall discuss briefly some of the characteristic features of ferromagnetic behavior in the two temperature regions.

(i) $T > \theta_f$. In the region above the ferromagnetic Curie temperature, the behavior of a ferromagnetic material is somewhat similar to that of a paramagnetic material. Thus, there exists a unique relationship between B and H, and between M and H. One can thus define the susceptibility $\chi = M/H = \mu_r - 1$, where χ and μ_r have a definite meaning. In this region, the susceptibility depends on temperature in accordance with the so-called *Curie-Weiss law*

$$\chi = \mu_r - 1 = C/(T - \theta) \qquad \text{for} \qquad T > \theta_f \tag{4.72}$$

C is called the *Curie constant;* θ is the *"paramagnetic" Curie temperature.* This expression is not valid in the region close to θ_f, as may be seen from Fig. 4.20; note that in this figure $1/\chi$ is plotted as a function of T. Comparison of Fig. 4.20 and Fig. 4.19 shows that the ferromagnetic case and the paramagnetic case are very similar; the only difference is that for a

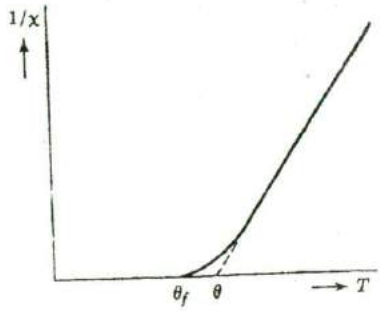

Fig. 4.20. The reciprocal of the susceptibility as a function of temperature for a ferromagnetic material above the ferromagnetic Curie temperature, θ_f. The paramagnetic Curie temperature θ is obtained by extrapolation of the straight portion of the curve which satisfies the Curie-Weiss law.

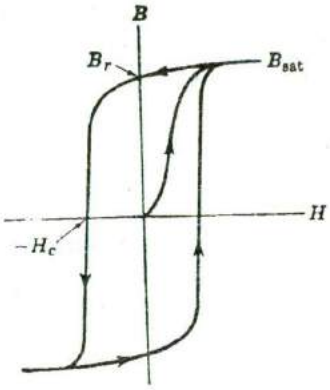

Fig. 4.21. Schematic representation of the hysteresis loop for a ferromagnetic material. The virgin curve starts at the origin.

truly paramagnetic material $\theta = 0$. The paramagnetic Curie temperature θ is usually somewhat higher than the ferromagnetic Curie temperature (see Fig. 4.20); for the ferromagnetic elements of the iron group, for example, these temperatures are, in degrees absolute:

	Fe	Co	Ni
θ_f . . .	1043	1393	631
θ . . .	1093	1428	650

(ii) $T < \theta_f$. Below the ferromagnetic Curie temperature, ferromagnetic materials exhibit the well-known *hysteresis* in the B versus H curves. A schematic representation of this behavior is given in Fig. 4.21. Starting with a virgin specimen, B varies reversibly with H for small fields. Since there is no hysteresis in this region, one defines the "*initial*" *permeability* μ_r in the same way as the permeability of a paramagnetic material. As the field H is increased, B begins to increase rapidly and ultimately approaches a saturation value B_{sat}. Along the virgin curve, one can still speak of a *differential permeability* defined by $1 + (dM/dH)$, but evidently this value is a function of H itself. The differential permeability may become very large, as is evident from the values given in Table 4.5 for high-permeability materials. Upon reducing the value of H from the saturation region to zero, it is observed that there remains a flux density B_r (*remanent flux density*). Since $H = 0$, the material must be spon-

taneously magnetized; in fact, the magnetization corresponding to B_r is equal to $M_r = B_r/\mu_0$. The occurrence of *spontaneous magnetization* is characteristic of ferromagnetic materials; in this respect they behave in a way similar to ferroelectrics.

The field $-H_c$ required to reduce the flux density to zero is called the *coercive force*. The coercive force of ferromagnetic materials varies over a wide range of values. For example, the coercive force of supermalloy, used in pulse transformers, is approximately 1 ampere m^{-1}, whereas that for a high stability permanent magnet may be as high as 10^6 ampere m^{-1}. The coercive force thus determines to a large extent the practical applications for which a given material may be used. Some data referring to the magnetic properties of a number of ferromagnetic materials are given in Table 4.5.

Table 4.5. SOME DATA PERTAINING TO FERROMAGNETIC MATERIALS (B_{sat} is the saturation flux density; B_r is the remanent flux density; H_c is the coercive force and $(\mu_r)_{max}$ is the maximum differential permeability.)

High permeability materials	$(\mu_r)_{max}$	B_{sat} (weber m^{-2})	H_c (amp m^{-1})
Iron	5000	2.1	80
4% Si-Fe	7000	2.0	40
Mu metal	10^5	0.65	4
Supermalloy	8×10^5	0.8	0.16

Permanent magnet materials	B_r (weber m^{-2})	H_c (amp m^{-1})
Carbon steel	1	4000
Alnico V	1.25	44,000
Platinum-Cobalt	0.45	2×10^5

4.11 Spontaneous magnetization and the Curie-Weiss law

In this section we shall discuss the atomic interpretations of spontaneous magnetization and of the Curie-Weiss law. Before doing this, we wish to point out that a piece of valuable information regarding the interpretation of ferromagnetic behavior may be gained by considering the magnitude of the remanent flux density of permanent magnets. We see from Table 4.5 that $B_r \approx 1$ weber m^{-2} for these materials, and since $H = 0$ we conclude that the remanent magnetization $M_r = B_r/\mu_0 \approx 10^6$ ampere m^{-1}. On the other hand, we know that an atomic dipole is of the order of 1 Bohr magneton, i.e. $\cong 10^{-23}$ ampere m^2. We thus require ap-

proximately 10^{29} atomic dipoles per m^3, all lined up in parallel, to obtain the observed magnetization. However, the number of atoms in a solid is approximately 10^{29} per m^3, so that the observed M, indicates *parallel alignment of essentially all the dipoles in the material.* This notion brings us to the first hypothesis of Weiss, who by 1907 had already suggested that in ferromagnetic materials the internal field seen by a given dipole is equal to the applied field plus a contribution from the neighboring dipoles which tends to align it in the same direction as its neighbors. Weiss expressed this mathematically by stating that the internal field $\mathbf{H}_i$ is given by*

$$\mathbf{H}_i = \mathbf{H} + \gamma\mathbf{M} \tag{4.73}$$

$\mathbf{H}$ is the applied field and $\gamma\mathbf{M}$ is a measure for the tendency of the environment to align a given dipole parallel to the magnetization already existing. The proportionality constant γ is the *internal field constant;* it determines the strength of the interaction between the dipoles (see the classification of magnetic materials in Table 4.1). We shall now show that a field of the type (4.73) is consistent with (a) the Curie-Weiss law and, (b) the occurrence of spontaneous magnetization. As a model we shall again consider a system of N spins per m^3, each giving rise to a magnetic moment of 1 Bohr magneton, β, either parallel or antiparallel to an external field. The magnetization of such a system may be obtained immediately from expression (4.69) for the paramagnetic case, by replacing H by H_i. Hence,

$$M = N\beta \tanh\left[\frac{\mu_0\beta}{kT}(H + \gamma M)\right] \tag{4.74}$$

At this point it is convenient to distinguish between two temperature regions:

(i) **High temperatures.** At sufficiently high temperatures, the term in square brackets in (4.74) will become small compared to unity. Then, since $\tanh x \cong x$ for $x \ll 1$, we may approximate (4.74) by

$$M = (N\mu_0\beta^2/kT)(H + \gamma M) \tag{4.75}$$

Solving this equation for M, one finds for the susceptibility of the material

$$\chi = \frac{M}{H} = \frac{N\mu_0\beta^2/k}{T - N\mu_0\beta^2\gamma/k} = \frac{C}{T - \theta} \tag{4.76}$$

Note that this expression is identical in form with the Curie-Weiss law (4.72). For the model studied here, we have

$$C = N\mu_0\beta^2/k \qquad \text{and} \qquad \theta = \gamma C \tag{4.77}$$

* Compare expression (2.32) for the case of dielectrics.

Since C and θ can be determined from measurements of the susceptibility as a function of temperature, the internal field constant γ can be calculated. One finds for ferromagnetic materials $\gamma \approx 10^3$. This value is about a thousand times as large as one would obtain on the assumption that the internal field is due to the *magnetic* interaction of the atomic dipoles (see problem 4.11). In fact, the forces acting between the dipoles in a ferromagnetic material cannot be explained in terms of classical physics; they are due to the wave nature of the electrons and in wave mechanics are called *exchange forces*.

(ii) **Spontaneous magnetization below the Curie temperature.** It follows from (4.76) that the Curie-Weiss law can hold only for temperatures $T > \theta$, because for $T = \theta$ the susceptibility would become infinite. This fact suggests already that at $T = \theta$, spontaneous magnetization may occur (non-vanishing M for $H = 0$); this is confirmed by the following arguments. In (4.74) let us put $H = 0$, and ask the question as to whether that equation permits a non-vanishing value for M. It is convenient to introduce a new variable

$$x = \gamma\mu_0\beta M/kT \tag{4.78}$$

so that (4.74) may be written (with $H = 0$) in the form

$$M/N\beta = M/M_{sat} = \tanh x \tag{4.79}$$

Here, $M_{sat} = N\beta$ represents the saturation value of the magnetization, since it gives the magnetization for parallel alignment of all the dipoles, and is evidently the maximum value that can be obtained. A plot of M/M_{sat}

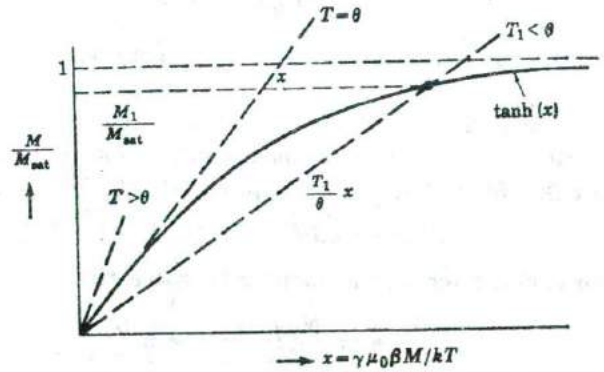

Fig. 4.22. Schematic illustration of the graphical solution of equation (4.79) for the spontaneous magnetization. For the temperature $T_1 (< \theta)$ the value of M_1/M_{sat} is obtained from the intersection of the line $(T_1/\theta)x$ and the $\tanh(x)$ curve. For $T \gg \theta$ the spontaneous magnetization vanishes.

as function of x is given in Fig. 4.22. According to (4.78), we should also have

$$\frac{M}{M_{sat}} = \frac{M}{N\beta} = \frac{kT}{N\gamma\mu_0\beta^2}\, x = \frac{T}{\theta}\, x \tag{4.80}$$

where the last equality follows from (4.77). Now, for a given temperature T, (4.80) in a plot of M/M_{sat} versus x represents a straight line with a slope equal to T/θ. Since M/M_{sat} must satisfy both (4.79) and (4.80), the value of M/M_{sat} for the temperature T is given by the intersection of the straight line and the tanh x curve, as indicated in Fig. 4.22. When this procedure is repeated for different temperatures, one can finally plot M/M_{sat} as function of T/θ, as shown in Fig. 4.23. Note that for $T \gtrsim \theta$, the spon-

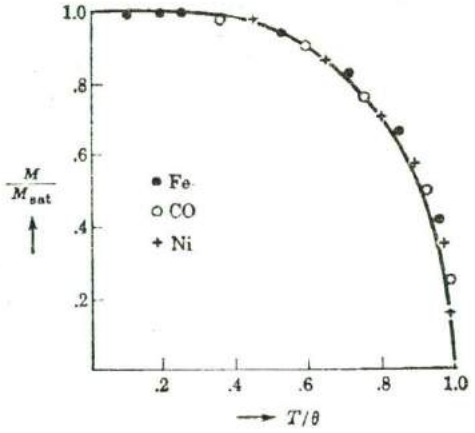

Fig. 4.23. The curve represents the relative spontaneous magnetization as a function of T/θ obtained from the procedure illustrated in Fig. 4.22. The points represent measured values for nickel, cobalt, and iron.

taneous magnetization vanishes. The reason for this can be seen in Fig. 4.22. When $T = \theta$, expression (4.80) gives $M/M_{sat} = x$, but this line is just the tangent of the tanh x curve at the point $x = 0$. For $T \gtrsim \theta$, the only intersection between (4.80) and (4.79) is the point $x = 0$; i.e., there is no longer a spontaneous magnetization. In Fig. 4.23, experimental points have been indicated, and the agreement with the theoretical curve is seen to be quite good. The reader should realize that the materials for which the experimental points have been plotted have widely different θ and M_{sat} values, as indicated in Table 4.6. The spontaneous magnetization becomes equal to M_{sat} only at $T = 0$, but it is evident from the curve in

Table 4.6. SATURATION VALUE OF THE SPONTANEOUS MAGNETIZATION AND FERROMAGNETIC CURIE TEMPERATURES FOR THE FERROMAGNETIC METALS

Metal	M_{sat} (amp m^{-1})	Curie temp. (°K)
Fe	1.75×10^6	1043
Co	1.45×10^6	1393
Ni	0.51×10^6	631

Fig. 4.23 that for iron and cobalt even at room temperature, the spontaneous magnetization is nearly equal to M_{sat}.

It is noted that the theory given predicts the same value for the ferromagnetic Curie temperature as for the paramagnetic Curie temperature, whereas experimental values of θ_f and θ differed somewhat. This discrepancy between theory and experiment must be ascribed to the simple form of the internal field expressed by (4.73). On the other hand, it must be admitted that this simple equation explains the spontaneous magnetization and the Curie law satisfactorily as far as the essential features are concerned.

4.12 Ferromagnetic domains and coercive force

After the discussion in the preceding section, the question may be raised as to how one can explain the fact that a piece of iron may not exhibit a resultant magnetization, and how one can explain the hysteresis in the B versus H curves of ferromagnetic materials. This brings us to the *second hypothesis of Weiss*. According to Weiss, a virgin specimen of iron consists of a number of regions or *domains* ($\approx 10^{-6}$ m or larger) which are spontaneously magnetized in accordance with the formulas derived in the preceding section. However, the *direction of the spontaneous magnetization varies from domain to domain*, and consequently, the resultant magnetization may be zero or nearly zero; this is indicated by the domain configuration in Fig. 4.24(a). If an external field H is applied, the domains with the proper direction of spontaneous magnetization grow at the expense of those that are magnetized in other directions by virtue of a motion of the domain walls [see Fig. 4.24(b)]. Ultimately, as the field is increased, the whole specimen may become one single domain, and saturation has been achieved. Thus, the hysteresis curve is associated with the motion of domain walls and, to some extent by domain rotation. The latter takes place as a result of the fact that spontaneous magnetization occurs only along certain directions in the crystal; when a field is applied in another arbitrary direction, the magnetization will rotate from an "easy"

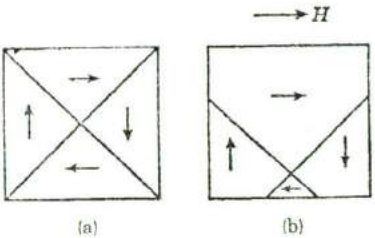

Fig. 4.24. The domain configuration in (a) has zero resultant magnetization. In (b) a magnetic field has been applied and the domain walls have moved so as to produce a net magnetization along the applied field direction.

direction to a "hard" direction. Since the hysteresis loop is interpreted in terms of domain wall motion, the coercive force must be determined by the "mobility" of the walls. The mobility of the domain walls is in turn determined by impurities, lattice imperfections, etc. and to some extent it is possible to "design" materials which require a large or a small coercive force. It may be mentioned here that the well-known Barkhausen effect is due to irregular fluctuations in the motion of domain walls; in earlier days, the effect had been ascribed to rotation of domains.

The most direct evidence for the existence of domains is provided by the so-called *Bitter powder patterns*. A drop of a colloidal suspension of ferromagnetic particles is placed on a well-prepared surface of the specimen; since there are strong local magnetic fields near the domain boundaries, the particles congregate there and the domain structure may be observed under a microscope.

4.13 Antiferromagnetic materials

In the discussion of ferromagnetic materials it was pointed out that the tendency for parallel alignment of the electron spins was due to quantum mechanical exchange forces. In certain materials, for example when the distance between the interacting atoms is small, the exchange forces produce a tendency for *antiparallel alignment* of electron spins of neighboring atoms. This kind of interaction is encountered in antiferromagnetic and in ferrimagnetic materials. It is of interest to note that certain properties of antiferromagnetic materials were predicted before antiferromagnetism was discovered experimentally. Thus, Néel and Bitter in the thirties made a theoretical study of the properties of antiferromagnetic models, and a few years later, in 1938, antiferromagnetism was discovered in MnO by Bizette, Squire and Tsai. Since that time, a number of other materials has been found to be antiferromagnetic. From the experimental point of view, the most characteristic feature of an antiferromagnetic material is the occurrence of a rather sharp maximum

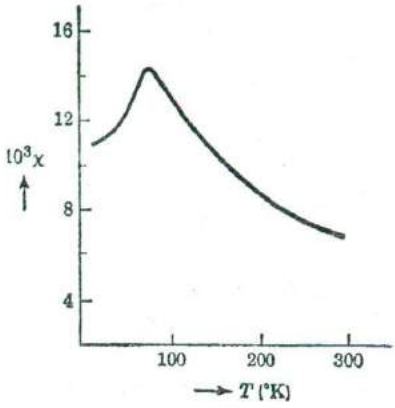

Fig. 4.25. The susceptibility of MnF_2 (polycrystalline) as a function of temperature. The maximum is characteristic of an antiferromagnetic transition. [After de Haas, Schultz, and Koolhaas, *Physica*, 7, 57 (1940)]

in the susceptibility-versus-temperature curve, as may be seen from the example given in Fig. 4.25 for MnF_2. The temperature for which this maximum occurs is called the *Néel temperature*, T_N. The Néel temperature plays a similar role in antiferromagnetic materials as does the ferromagnetic Curie temperature in ferromagnetic materials. Thus, above the Néel temperature, the susceptibility is observed to follow the equation

$$\chi = \frac{C}{T + \theta} \tag{4.81}$$

where C is the Curie constant and θ the paramagnetic Curie temperature. Below the Néel temperature, the spin system tends to be "ordered" in a way similar to the spin system in a ferromagnetic material, except that at $T = 0$ half the spins are oriented in one direction and the other half in the opposite direction. Confining ourselves for the moment to the high temperature region, it is of interest to recapitulate the results for the susceptibility versus temperature behavior for para-, ferro-, and antiferromagnetic materials:

para-	*ferro-*	*antiferro-*
$\chi = C/T$	$\chi = C/(T - \theta)$ for $T > \theta_f$	$\chi = C/(T + \theta)$ for $T > T_N$

(4.82)

The difference between the three groups of materials is illustrated in Fig. 4.26 in terms of a plot of $1/\chi$ versus temperature.

We shall now consider a simple model of an antiferromagnetic material. With reference to Fig. 4.27, consider a body centered cubic lattice. We shall distinguish in this lattice between A-sites and B-sites, as indicated in Fig. 4.27. Each A-site is surrounded by eight B-sites, and each

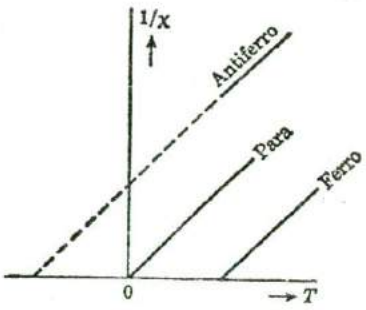

Fig. 4.26. Illustrating the reciprocal susceptibility as a function of temperature for a paramagnetic, ferromagnetic, and antiferromagnetic material.

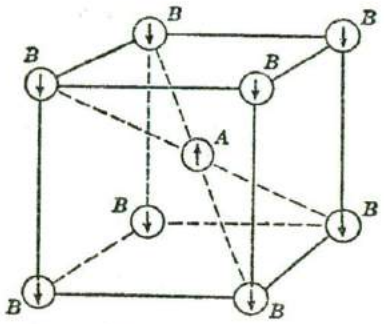

Fig. 4.27. Representation of two sub-lattices, A and B; the spins on the A-lattice tend to line up antiparallel to those on the B-lattice.

B-site is surrounded by eight A-sites. We shall assume that all sites are occupied by identical atoms with a magnetic dipole moment of 1 Bohr magneton which can orient itself either in the "up" or the "down" direction. Also, we shall assume that an atom at an A-site tends to align its spin opposite to the spins of the neighboring atoms on the B-sites, and vice versa. In order to describe this mathematically, we introduce an internal field $\mathbf{H}_a$ for the atoms on A-sites and an internal field $\mathbf{H}_b$ for the atoms on B-sites. Following a procedure similar to that used in section 4.11 for a ferromagnetic material, we may then write

$$\mathbf{H}_a = \mathbf{H} - \gamma \mathbf{M}_b \qquad \text{and} \qquad \mathbf{H}_b = \mathbf{H} - \gamma \mathbf{M}_a \tag{4.83}$$

Here, $\mathbf{M}_a$ and $\mathbf{M}_b$ represent the magnetizations of the A-sub-lattice and of the B-sub-lattice respectively. The minus signs represent the assumption that an A atom tends to align its dipole moment opposite to the direction of the magnetization of the B-lattice; the internal field constant γ determines the strength of the exchange interaction. The magnetizations M_a and M_b may be obtained again from formula (4.69) by replacing H by the appropriate internal fields. Hence, if there are N atoms per m^3 on the A-lattice and an equal number of atoms on the B-lattice, we find

$$\begin{aligned} M_a &= N\beta \tanh\left[\frac{\mu_0\beta}{kT}(H - \gamma M_b)\right] \\ M_b &= N\beta \tanh\left[\frac{\mu_0\beta}{kT}(H - \gamma M_a)\right] \end{aligned} \tag{4.84}$$

At sufficiently high temperatures, we may make use of the fact that

$\tanh \cong x$ for $x \ll 1$, so that then (4.84) reduces to

$$\begin{aligned} \mathbf{M}_a &= (N\beta^2\mu_0/kT)(\mathbf{H} - \gamma\mathbf{M}_b) \\ \mathbf{M}_b &= (N\beta^2\mu_0/kT)(\mathbf{H} - \gamma\mathbf{M}_a) \end{aligned} \tag{4.85}$$

The total magnetization of the material is given by

$$\mathbf{M} = \mathbf{M}_a + \mathbf{M}_b \tag{4.86}$$

and consequently may be calculated by adding the two (4.85) equations; this gives

$$\mathbf{M} = (N\mu_0\beta^2/kT)(2\mathbf{H} - \gamma\mathbf{M}) \tag{4.87}$$

Since the net magnetization M must have the same direction as H, we may consider (4.87) as a scalar equation. Solving for M/H we thus find for the susceptibility at high temperatures

$$\chi = M/H = 2C/(T + \gamma C) = 2C/(T + \theta) \tag{4.88}$$

where $C = N\mu_0\beta^2/k$ and $\theta = \gamma C$

Note that this model indeed gives a susceptibility as required by the experimentally derived equation (4.81).

At low temperatures, the approximation involved in going from (4.84) to (4.85) is no longer justified. In fact, at $T = 0$, the spin system is completely ordered in the sense that all spins on A-sites are oriented in parallel and all spins on the B-sites are oriented in parallel. Thus, at low temperatures, $\mathbf{M}_a$ amd $\mathbf{M}_b$ are very large, though oppositely directed. As the temperature is raised from zero, the magnetizations M_a and M_b of the two sub-lattices in the absence of a magnetic field vary with temperature in a fashion similar to the spontaneous magnetization of a ferromagnetic material. The spontaneous magnetizations of the sub-lattices disappears at the Néel temperature T_N. We shall not discuss here the solution of equation (4.84) for the temperature region below T_N; it may suffice to say that the behavior of the experimentally observed susceptibility curve (see Fig. 4.25) can be understood in terms of the model under discussion. However, we may discuss here the occurrence of a Néel temperature for the model. This can be done on the basis of the simpler formulas (4.85), because at the Néel temperature itself the spontaneous magnetization of the sub-lattices vanishes, as can be seen from Fig. 4.23; i.e., at the Néel temperature itself formulas (4.85) should still be valid. Let us investigate then, by putting $H = 0$ in (4.85), for what temperature spontaneous magnetization of the sub-lattices becomes possible. Rewriting (4.85) for

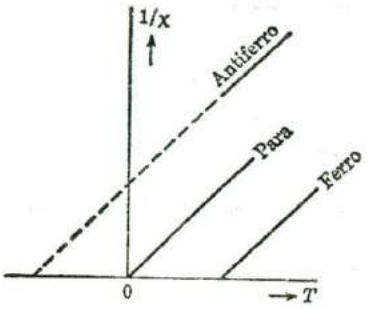

Fig. 4.26. Illustrating the reciprocal susceptibility as a function of temperature for a paramagnetic, ferromagnetic, and antiferromagnetic material.

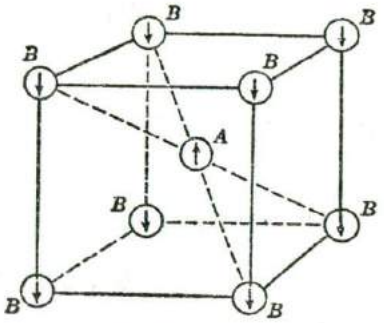

Fig. 4.27. Representation of two sub-lattices, A and B; the spins on the A-lattice tend to line up antiparallel to those on the B-lattice.

B-site is surrounded by eight A-sites. We shall assume that all sites are occupied by identical atoms with a magnetic dipole moment of 1 Bohr magneton which can orient itself either in the "up" or the "down" direction. Also, we shall assume that an atom at an A-site tends to align its spin opposite to the spins of the neighboring atoms on the B-sites, and vice versa. In order to describe this mathematically, we introduce an internal field $\mathbf{H}_a$ for the atoms on A-sites and an internal field $\mathbf{H}_b$ for the atoms on B-sites. Following a procedure similar to that used in section 4.11 for a ferromagnetic material, we may then write

$$\mathbf{H}_a = \mathbf{H} - \gamma \mathbf{M}_b \qquad \text{and} \qquad \mathbf{H}_b = \mathbf{H} - \gamma \mathbf{M}_a \tag{4.83}$$

Here, $\mathbf{M}_a$ and $\mathbf{M}_b$ represent the magnetizations of the A-sub-lattice and of the B-sub-lattice respectively. The minus signs represent the assumption that an A atom tends to align its dipole moment opposite to the direction of the magnetization of the B-lattice; the internal field constant γ determines the strength of the exchange interaction. The magnetizations M_a and M_b may be obtained again from formula (4.69) by replacing H by the appropriate internal fields. Hence, if there are N atoms per m^3 on the A-lattice and an equal number of atoms on the B-lattice, we find

$$M_a = N\beta \tanh\left[\frac{\mu_0\beta}{kT}(H - \gamma M_b)\right]$$

$$M_b = N\beta \tanh\left[\frac{\mu_0\beta}{kT}(H - \gamma M_a)\right] \tag{4.84}$$

At sufficiently high temperatures, we may make use of the fact that

$\tanh \cong x$ for $x \ll 1$, so that then (4.84) reduces to

$$\begin{aligned} \mathbf{M}_a &= (N\beta^2\mu_0/kT)(\mathbf{H} - \gamma\mathbf{M}_b) \\ \mathbf{M}_b &= (N\beta^2\mu_0/kT)(\mathbf{H} - \gamma\mathbf{M}_a) \end{aligned} \tag{4.85}$$

The total magnetization of the material is given by

$$\mathbf{M} = \mathbf{M}_a + \mathbf{M}_b \tag{4.86}$$

and consequently may be calculated by adding the two (4.85) equations; this gives

$$\mathbf{M} = (N\mu_0\beta^2/kT)(2\mathbf{H} - \gamma\mathbf{M}) \tag{4.87}$$

Since the net magnetization M must have the same direction as **H**, we may consider (4.87) as a scalar equation. Solving for M/H we thus find for the susceptibility at high temperatures

$$\chi = M/H = 2C/(T + \gamma C) = 2C/(T + \theta) \tag{4.88}$$

where $C = N\mu_0\beta^2/k$ and $\theta = \gamma C$

Note that this model indeed gives a susceptibility as required by the experimentally derived equation (4.81).

At low temperatures, the approximation involved in going from (4.84) to (4.85) is no longer justified. In fact, at $T = 0$, the spin system is completely ordered in the sense that all spins on A-sites are oriented in parallel and all spins on the B-sites are oriented in parallel. Thus, at low temperatures, $\mathbf{M}_a$ amd $\mathbf{M}_b$ are very large, though oppositely directed. As the temperature is raised from zero, the magnetizations M_a and M_b of the two sub-lattices in the absence of a magnetic field vary with temperature in a fashion similar to the spontaneous magnetization of a ferromagnetic material. The spontaneous magnetizations of the sub-lattices disappears at the Néel temperature T_N. We shall not discuss here the solution of equation (4.84) for the temperature region below T_N; it may suffice to say that the behavior of the experimentally observed susceptibility curve (see Fig. 4.25) can be understood in terms of the model under discussion. However, we may discuss here the occurrence of a Néel temperature for the model. This can be done on the basis of the simpler formulas (4.85), because at the Néel temperature itself the spontaneous magnetization of the sub-lattices vanishes, as can be seen from Fig. 4.23; i.e., at the Néel temperature itself formulas (4.85) should still be valid. Let us investigate then, by putting $H = 0$ in (4.85), for what temperature spontaneous magnetization of the sub-lattices becomes possible. Rewriting (4.85) for

$H = 0$ we obtain

$$M_a + \frac{C}{T}\gamma M_b = 0$$
$$\frac{C}{T}\gamma M_a + M_b = 0 \tag{4.89}$$

For $T > T_N$, these equations have the trivial solutions $M_a = M_b = 0$; i.e., there is no spontaneous magnetization of the sub-lattices above the Néel temperature. If spontaneous magnetization of the sub-lattices is supposed to set in for $T = T_N$, we must require that (4.89) has non-trivial solutions for M_a and M_b at the temperature $T = T_N$. This permits us to calculate T_N, because the requirement just stated is equivalent to the requirement that the determinant of the coefficients of M_a and M_b vanishes. Hence

$$\left(\frac{C}{T_N}\gamma\right)^2 = 1 \quad \text{or} \quad T_N = C\gamma = \theta \tag{4.90}$$

where the last relationship follows from (4.88). Note that for the model employed here, the Néel temperature turns out to be the same as the paramagnetic Curie temperature θ. (The reader is reminded of the fact that in the ferromagnetic case the simple model employed also gave $\theta_f = \theta$.) According to measurements of θ and T_N, there is a considerable difference between T_N and θ, as may be seen from Table 4.7. This indicates that the model used here was actually too simple. In fact, one can show that if one takes into account antiferromagnetic interactions not only between nearest neighbors, but also between next nearest neighbors, the model above would give $T_N < \theta$. The model discussed here must therefore be considered as an approximation; it predicts the general features of antiferromagnetism correctly, but not the details. It should also be realized that usually the particular body-centered structure assumed in Fig. 4.27 does not apply to the material under study. In Table 4.7 we give values of T_N and θ for some antiferromagnetic materials.

The question can be raised as to what independent experimental evidence there exists to support the assumption that in an antiferromagnetic material neighboring spins have opposite directions. The answer is that such evidence has been obtained from *neutron diffraction studies*. The neutrons, because of their magnetic moment, can "see" the difference between an "up" spin and a "down" spin and the diffraction patterns (similar to X-ray diffraction patterns) show that the antiparallel spin alignment actually occurs in these materials.

Table 4.7. NÉEL TEMPERATURE (T_N) AND PARAMAGNETIC CURIE TEMPERATURE (θ) FOR SOME ANTIFERROMAGNETIC MATERIALS

Material	T_N(°K)	θ(°K)
MnF_2	72	113
MnO_2	84	316
MnO	122	610
MnS	165	528
FeO	198	570
NiF_2	73	116
CoO	292	280

4.14 Ferrimagnetic materials

Of the ferrimagnetic materials, the so-called *ferrites* are of greatest interest from the electrical engineering point of view; they behave as ferromagnetic materials in as much as they show spontaneous magnetization below a certain temperature. As far as their conductivity is concerned, they behave as semiconductors. The d-c resistivity of ferrites is many orders of ten higher than that of iron; consequently, the eddy current problem preventing penetration of magnetic flux into the material is much less severe in ferrites than in iron. Ferrites can therefore be used for frequencies up to microwaves in transformer cores and are of great technical importance in this respect.

The chemical formula of simple ferrites may be written as $Me^{2+}Fe_2^{3+}O_4^{2-}$, where Me^{2+} may represent a variety of divalent metallic ions, such as Fe^{2+}, Co^{2+}, Mn^{2+}, Zn^{2+}, Cd^{2+}, Mg^{2+}, etc. Symbolically, one may write the formula as a "mixture" of MeO and Fe_2O_3, although a ferrite is actually a solid solution of two such oxides.

Since the oxides contain ions, the magnetic properties should be predictable to a good degree of approximation from the magnetic properties of the ions. Thus, from Table 4.3 we expect, for example, each Fe^{2+} ion to correspond to 4 Bohr magnetons, and each Fe^{3+} to 5 Bohr magnetons. Now, a material such as $Fe^{2+}Fe_2^{3+}O_4^{2-}$ exhibits a saturation magnetization which amounts to 4β (β = 1 Bohr magneton) per "molecule" $Fe^{2+}Fe_2^{3+}O_4^{2-}$. It is evident that if the spins of all the ions were lined up in parallel one should find $4 + (2 \times 5) = 14$ Bohr magnetons per molecule. This discrepancy was explained in 1948 by Néel in terms of a model consisting of two sub-lattices, somewhat similar to the AB lattice in Fig. 4.27, for which he assumed an antiferromagnetic interaction between A-sites and B-sites. An important role in this interpretation is played by studies of the atomic

arrangement in ferrites, from which it has been possible to identify the A- and B-sites.

Because of the intimate relationship between the magnetic properties of ferrites and the crystal structures of ferrites, a few remarks may be made here concerning this problem. The oxygen ions in a ferrite form a close-packed face-centered cubic structure. In this arrangement it is found that for every four O^{2-} ions, there are two *octahedral* "holes" (surrounded by six O^{2-} ions) and 1 *tetrahedral* "hole" (surrounded by four O^{2-} ions). The metal ions are distributed over these octahedral and tetrahedral sites. The tetrahedral sites may be identified with the A-sites, and the octahedral sites with the B-sites mentioned earlier. Thus, the octahedral sub-lattice has twice as many sites as the tetrahedral one. This has been represented schematically in Fig. 4.28. Now, in $Fe^{2+}Fe_2^{3+}O_4^{2-}$

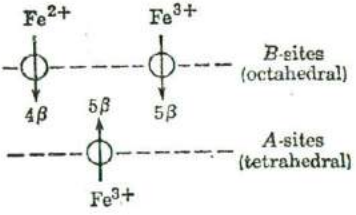

Fig. 4.28. Schematic representation of Fe^{2+} and Fe^{3+} ions in magnetite. There are two Fe^{3+} ions and one Fe^{2+} ion per molecule of Fe_3O_4, as indicated. The net moment per molecule is 4β.

(magnetite), for example, the Fe^{2+} ions occupy half of the octahedral sites; the Fe^{3+} ions occupy the other half of the octahedral sites, and the tetrahedral sites (see Fig. 4.28). Hence, if there exists an antiferromagnetic interaction between A- and B-sites, we see from Fig. 4.28 that the Fe^{3+} magnetic moments just cancel each other, so that the magnetization of Fe_3O_4 should be equal to that produced by the Fe^{2+} ions alone, i.e. 4β per molecule; that is in agreement with experiment.

The behavior of other ferrites may be explained in similar terms. We may mention here an interesting feature of ferrites, which shows again the importance of the atomic arrangement for the properties of these materials: it is observed that if in Fe_3O_4, some of the magnetic Fe^{2+} ions are replaced by non-magnetic ions such as Zn^{2+} or Cd^{2+}, the magnetization increases! The reason for this peculiar behavior is the following: Zinc ions go preferably into tetrahedral positions, thereby forcing some of the Fe^{3+} ions from tetrahedral to octahedral sites. Since the Zn^{2+} ions have no magnetic dipole moment, the net magnetization increases, as may be seen from Fig. 4.29. It will be evident that these materials lend themselves,

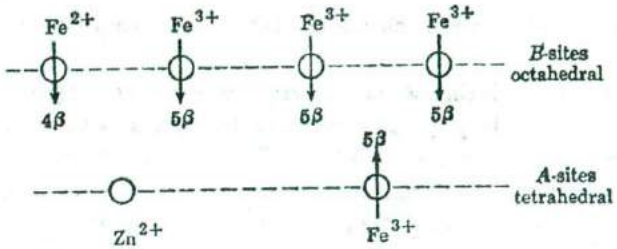

Fig. 4.29. Schematic representation of the ionic distribution in magnetite after replacing half of the Fe^{2+} ions by Zn^{2+}. The Zn^{2+} ions prefer tetrahedral positions and force Fe^{3+} ions to move into octahedral sites.

within certain limits, to designing materials with prescribed spontaneous magnetization.

References

L. F. Bates, *Modern Magnetism*, 3d ed., Cambridge, London, 1951.

E. W. Gorter, "Saturation Magnetization and Crystal Chemistry of Ferrimagnetic Oxides," *Philips Research Reports*, **9**, 295, 321, 403 (1954); see also *Proc. IRE*, **43**, 1945 (1955).

J. L. Snoek, *New Developments in Ferromagnetic Materials*, Elsevier, New York, 1947.

J. van den Handel, "Paramagnetism," *Advances in Electronics and Electron Physics*, 6, 463 (1954).

Problems

4.1 A linear conductor carries a current of 10 amperes along the positive x-direction. Find the force per meter length on the conductor if it is subjected to a homogeneous flux density of 0.5 weber m^{-2} along the z-direction.

4.2 A linear conductor in air carries a current of 5 amperes; calculate the flux density produced by 1 cm of the conductor in a point at a distance of 1 m normal to the 1 cm section.

4.3 Show by means of Biot and Savart's law that the flux density produced by an infinitely long straight wire, carrying a current I, in a point at a distance a normal to the wire is given by $\mu_0\mu_r I/2\pi a$.

4.4 Two infinite parallel conductors carry parallel currents of 10 amperes each. Find the magnitude and direction of the force between the conductors per meter length if the distance between them is 20 cm.

4.5 An electron with velocity vector v moves in combined electric and magnetic fields **E** and **B**. Write down the expression for the force on the electron (the "Lorentz force").

4.6 Show that an electron with a velocity perpendicular to the direction of a homogeneous magnetic field of flux density B describes a circular path with an angular velocity of rotation equal to eB/m.

4.7 A charge of e coulombs is distributed homogeneously over the surface of a sphere of radius R meters. The sphere rotates with an angular velocity ω about an axis passing through its center. Show that the magnetic dipole moment of the sphere is equal to $\frac{1}{3}e\omega R^2$. Also show that the angular momentum of the sphere is $\frac{2}{3}m\omega R^2$, where m is the total mass of the charge.

4.8 Consider a charge of e coulombs distributed homogeneously over the surface of a sphere of radius R meters. If the sphere is initially at rest, show that after application of a flux density of B weber m^{-2}, the charge distribution will rotate with an angular velocity $\boldsymbol{\omega} = (e/2m)\mathbf{B}$, where m is the total mass of the charge.

4.9 The magnetic field strength in a piece of copper is 10^6 ampere m^{-1}. Given that the magnetic susceptibility of copper is -0.5×10^{-5}, find the flux density and the magnetization in the copper.

4.10 The magnetic field strength in a piece of Fe_2O_3 is 10^6 ampere m^{-1}. Given that the susceptibility of Fe_2O_3 at room temperature is 1.4×10^{-3}, find the flux density and the magnetization in the material; compare the answers with those of the preceding problem. What is the magnetization at the temperature of liquid nitrogen?

4.11 Consider two point dipoles, each with a strength of 1 Bohr magneton; the dipoles are parallel to each other and parallel to the line joining their centers. If the distance between the dipoles is 2 angstrom, calculate the energy of one dipole in the field of the other and show that the result is equivalent to kT with $T \approx 1°K$. (This shows that ferromagnetic interactions cannot be explained classically, because the interaction energy should be of the order of kT where $T = \theta_f \cong 1000°K$).

4.12 The saturation value of the magnetization of iron is 1.75×10^6 ampere m^{-1}. Given that iron has a body-centered cubic structure with an elementary cube edge of 2.86 angstroms, calculate the average number of Bohr magnetons contributed to the magnetization per atom.

4.13 A paramagnetic system of spins is subjected to a homogeneous field of 10^6 ampere m^{-1} at a temperature of 300°K. Find the average magnetic moment along the field direction per spin in Bohr magnetons. Answer the same question for liquid helium temperature.